NOVEL SPECTROSCOPIC TECHNIQUES USING THE PULSED GLOW DISCHARGE

By

WILLIAM OTIS WALDEN

A DISSERTATION PRESENTED TO THE GRADUATE SCHOOL
OF THE UNIVERSITY OF FLORIDA IN PARTIAL FULFILLMENT
OF THE REQUIREMENTS FOR THE DEGREE OF
DOCTOR OF PHILOSOPHY

UNIVERSITY OF FLORIDA

1995

To Endeavor

ACKNOWLEDGEMENTS

As my mentors, I have the highest regard for Dr. Willard W. Harrison and Dr. J. D. Winefordner. Specifically, I would like to thank Dr. Winefordner for stressing to me the basics of scientific research. I'm indebted to Dr. Harrison for his support and strengthening my artistic ability.

I will remember everyone in Dr. Harrison's and Dr. Winefordner's groups as good friends. They were always there to lend a hand or to offer a helpful suggestion. The closeness and cooperation between the shared groups has made my graduate years much more bearable. Dr. Ben Smith has offered me invaluable experience in instrumentation and theory and I appreciate the remarkable patience he showed.

Finally, this work would not have been possible without the appreciated support by the United States Department of Energy, Division of Chemical Sciences.

TABLE OF CONTENTS

Page

ACKNOWLEDGEMENTS iii

LIST OF FIGURES vi

ABSTRACT x

CHAPTERS

1 THE GLOW DISCHARGE AS A SPECTROSCOPIC SOURCE 1

- Historical Background 1
- Electric Discharges 5
- Glow Discharges 8
  - Plasma Initiation 12
  - Sputtering 14
  - Excitation 19
  - Modes of Operation 25
    - Direct current discharges 25
    - Radio frequency discharges 26
- Pulsed Glow Discharges 26
  - History 26
  - Pulse Characteristics 27
    - The prepeak 28
    - The plateau 28
    - The afterpeak 29

2 ATOMIC FLUORESCENCE SPECTROSCOPY 32

- History 32
- Theory 34
- Atomic Reservoirs 46

3 MULTIELEMENT GLOW DISCHARGE ATOMIC FLUORESCENCE........ 46

Introduction........ 46
Experimental........ 50
Xenon Arc Lamp........ 56
Xenon Flashlamp........ 60
Diagnostics........ 70
Analytical Usefulness........ 76

4 THE MICROSECOND PULSE GLOW DISCHARGE........ 83

Introduction........ 83
Experimental........ 85
MPGD Emission........ 88
Plasma Diagnostics........105
    Mass Spectrometry........108
    Temperature Measurements........112
    Atomic Absorption........117
    Diffusion Studies........120
Nonconductors........126

5 CONCLUSIONS........129

REFERENCES........134

BIOGRAPHICAL SKETCH........143

LIST OF FIGURES

Figure Page

1 Representation of a simple glow discharge.. 2

2 Relationship between voltage and current in gaseous discharges........... 6

3 Luminous zones within a glow discharge tube... 10

4 Potential drop across a glow discharge tube.. 11

5 Process by which incident ions sputter surface atoms............................. 16

6 Sputter yields for various elements... 22

7 Gas phase reactions in the negative glow.. 23

8 Profiles for the millisecond-pulsed glow discharge................................... 30

9 A two level system for fluorescence... 36

10 Pathways for excitation and de-excitation in a two level system.............. 37

11 Fluorescence curves for continuum and line sources............................... 39

12 Schematic of the GO-LEAFS experimental system.................................. 45

13 Xenon flashlamp emission spectrum... 48

14 Exploded view of the direct insertion probe cathode assembly..... 52

15 Schematic for multielement GDAFS using xenon lamps............................ 54

16 Glow discharge 58

17 Signal and S/B for the copper 324.7 nm line versus pressure.................. 61

18 Spatial profile of emission and fluorescence signals................................ 62

19 Copper 249.2 nm fluorescence profile and S/B for the pulsed GO............ 65

20 Fluorescence spectra at the initiation of the discharge............................ 66

21 Temporal profiles observed after discharge termination........................... 67

22 Copper emission spectrum using the xenon flashlamp........................... 69

23 Copper 324.7 nm fluorescence decay in NIST # 602.............................. 73

24 Aluminum 309.1 nm fluorescence decay in NIST # 602........................... 74

25 Magnesium 285.2 nm fluorescence decay in NIST # 602......................... 75

26 Aluminum NIST #602 fluorescence spectrum.. 77

27 Calibration curve for magnesium in aluminum standards......................... 78

28 Tantalum emission and fluorescence spectra.. 80

29 Steel NIST #462 emission and fluorescence spectra.............................. 81

30 Manganese fluorescence in Steel NIST# 462.. 82

31 Schematic diagram for optical spectroscopy with MPGD......................... 86

32 Current and voltage profiles for a ten microsecond pulse........................ 91

33 Current, voltage and signal after initiation.. 92

34 Profiles of various MPGD emission lines.. 94

35 MPGD temporal emission profiles... 95

36 Copper MPGD emission spectra for gated delay times............................ 96

37 Spatial intensity profiles for the copper 324.7 nm line.............................. 98

38 MPGD emission profile across a copper pin.. 99

39 MPGD copper 249.2 nm emission versus pressure...............................100

40 MPGD copper 249.2 nm emission versus frequency....102

41 MPGD copper 249.2 nm emission versus pulse width....103

42 MPGD Brass NIST #1109 fluorescence and emission spectra....106

43 Calibration curves for zinc in copper....107

44 Copper MPGD ion profiles versus extraction distance....109

45 MPGD/MS spectra for iron, NIST #661....111

46 MPGD N_2^+ emission, 10% N_2 in argon, 0.9 torr, 100 mW power....114

47 Boltzmann plot for the MPGD rotational temperature....115

48 MPGD absorption profiles for a 10 microsecond pulses....117

49 Peak absorbance plots at various power supply pulse widths....118

50 Sputter rate comparisons for the DC and MP modes....119

51 (A) MPGD absorption and emission profiles. (B) Profile for absorption after subtracting out emission....121

52 Copper fluorescence profiles at various boxcar delays....122

53 Copper 324.7 absorption profile versus distance from cathode....123

54 Uncorrected and calculated peak absorbance times....127

55 MPGD spectrum for MACOR....128

Abstract of Dissertation Presented to the Graduate School
of the University of Florida in Partial Fulfillment of the
Requirements for the Degree of Doctor of Philosophy

NOVEL SPECTROSCOPIC TECHNIQUES USING THE PULSED GLOW DISCHARGE

By

William Otis Walden

DECEMBER 1995

Co-Chairs: Willard W. Harrison and James D. Winefordner
Major Department: Chemistry

The glow discharge is a versatile atom source for the analytical chemist. This plasma produces atoms, ions, and excited species, allowing it to be used as a source for most traditional spectroscopic methods. The most attractive aspect of this source is that it can directly atomize almost any type of solid sample.

Analytical chemists continually search for the perfect method of analysis. This method would accommodate all sample types, have multielement capability require little or no sample preparation, be inexpensive, have low maintenance, and obtain low detection limits. Glow discharge atomic emission spectroscopy possesses the first five characteristics of a perfect method but falls short with its limits of detection.

This dissertation reports on two pulsed glow discharge methods designed to increase signal-to-background ratios over those found with direct current (DC) glow discharge emission. The first method involves the use of spectral continuum sources to promote multielement fluorescence. Both the xenon arc lamp and xenon flashlamp were used as sources. The lamps were found to induce selectively atomic fluorescence without exciting argon or molecular species. The best analytical spectra were obtained by sampling the atomic population with the xenon flashlamp, fired at the termination of a millisecond pulsed glow discharge.

The second method to improve the signal-to-noise was provided by a high powered, microsecond pulsed glow discharge. With this method, an increase of 50 to 500 times in the emission signal was observed compared with a DC glow discharge. The very short on-times of the microsecond discharge permitted diagnostic studies of diffusion and the evolution of certain plasma species.

CHAPTER 1
THE GLOW DISCHARGE AS A SPECTROSCOPIC SOURCE

Historical Background

A glow discharge (GD) is a modest plasma (10^{11} - 10^{13} atoms/cm^3), initiated upon the electrical breakdown of a low pressure rare gas across two electrodes.[1] A typical glow discharge tube is shown in Figure 1. It is an easily formed self-sustaining discharge that is maintainable at pressures around 1 torr, voltages up to 2 kV, and currents from 1 to 1000 mA. Glow discharges have been widely used for metal deposition in industry. This ability to produce an atomic vapor directly from a solid sample underlies its use as an analytical source.

Mainly, the GD allows the rapid trace elemental analysis of solids, bypassing the need for extensive sample preparation or dilution. The emission from a GD device was observed almost a century before its widespread acceptance into analytical spectroscopy.[2] Besides atomic emission spectroscopy (GDAES),[3,4,5] the atomic population produced from the GD can be measured using atomic absorption (GDAAS)[6,7,8] and fluorescence spectroscopy (GDAFS),[4,9] while the ions it produces are sampled by mass spectrometry (GDMS).[10,11]

The GD exhibits some unique spectroscopic characteristics with respect to

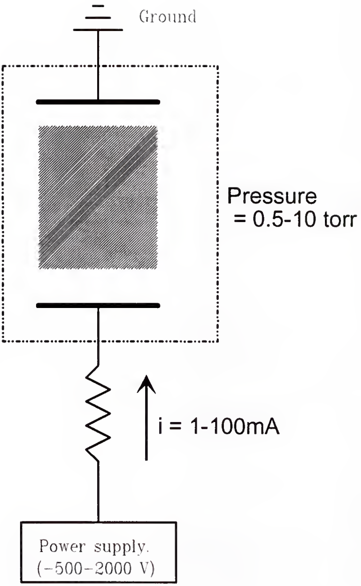

Fig. 1- Representation of a simple glow discharge.

other atomic reservoirs.[12] It is cool running (T ≈ 600K), temporally stable in atomic density, efficient in sputtering of metal atoms, and it contains atoms near to thermal equilibrium.[13] The sputtered population of this inert, low pressure argon plasma is not subject to molecular formation and quenching as opposed to atmospheric pressure sources. Also, the atomic population of the GD is not subject to many undesirable characteristics associated with these atomic reservoirs. Mainly, higher pressure sources, such as ICPs and flames, cause the quenching of excited states and collisional broadening of spectroscopic lines.

Glow discharges may be operated with a wide range of geometries, pressures, voltages, and currents. For all parameters, the GD exhibits a distinctive luminous zone (the negative glow), which is a site of atomic emission that represents the cathode material.[14] The negative glow is a good emission source for atomic spectroscopy.[15] Glow discharges have also been used as atom generators for spectroscopic methods.[16,17,18] These measurements have gained much popularity, since the GD was first sought as a reservoir for atomic absorption analysis in 1959.[19]

Although the GD is not a strong plasma (it has a ion population less than 50%), it does induce some ionization of the sputtered analyte atoms (~1%). This is sufficient for it to be utilized as a source for mass spectrometry.[20] Modern GDMS began when a direct current glow discharge (DC-GD) was coupled to a mass spectrometer, to examine ionic interactions within the plasma.[21] In the early 197Os, a radio frequency glow discharge (RF-GD) was the first type to be coupled to a mass spectrometer for trace analysis.[20,22] Consequently, the GD ion source has been interfaced with most types of mass spectrometer systems. Recently, a DC glow discharge has been joined to a Fourier transform ion cyclotron resonance (FTICR) mass analyzer with a resolution approaching 300,000.[23,24,25] GDMS possesses the ability to do elemental analyses on a variety of samples with good sensitivity.[26,27,28] The GD source has also been used to introduce liquid samples [29,30] and organic compounds into a mass spectrometer.[31]

The glow discharge is a low temperature plasma and most of its sputtered metal atoms are in their ground states or have only low lying energy levels populated. This makes it a good source for atomic measurements and has sparked an interest to use it as atom reservoir for ultratrace analysis of solutions. Harrison *et al.* analyzed solutions by drying them on the cathode of the glow discharge.[1] In addition to analytical determinations, fluorescence measurements are useful in fundamental studies of the GD though the monitoring of various plasma species.[32]

Modifications and applications for the GD have exploded in recent years. One of the most notable developments came through powering the GD with a RF supply to sputter nonconductors. Mass spectra for a glass sample with few molecular interferents have been obtained using an RF-GDMS system.[33] Much of the current research has shifted from optical spectroscopy to GDMS. This change in focus stems from mass spectrometry's higher sensitivity, fewer spectral interferences, and lower background. Alternatively, GDAES is still a common alternative to GDMS, because of its operational simplicity and low cost.

Electric Discharges

A gas discharge is a general term meaning the conduction of electricity through a gaseous medium, and the GD is just one type.[34] It is possible to produce gas discharges over a wide range of pressures and currents. Gaseous discharges are characterized according to the amount of current passing through them.[35] They are compared with respect to current and voltage in Figure 2.

There are three types of low pressure (0.1-10 Torr) gaseous discharges-the Townsend discharge, the glow discharge, and the arc discharge. These discharge types are defined by current as follows.

1) Townsend discharges have currents less than 10^{-6} amperes (A).

2) Glow discharges have currents between 10^{-6} to 1 A.

3) Arc discharges have currents greater than 1 A.

At high accelerating voltages, electrons acquire enough energy to ionize the fill gas between the electrodes. A Townsend discharge cannot sustain itself at less than 10^{-12} A without an outside source of electrons.[35] Gaseous discharges become self-sustaining when cathodic electrons produce several secondary electrons in the gas phase. The current at which a discharge becomes self-sustaining varies with many parameters, such as the voltage, the cathode material, the distance between the electrodes, and the type of fill gas used. Above all, it requires that the primary electrons, streaming from the cathode, ionize the fill gas (argon). In turn, the argon ions (Ar^+) accelerate in the electric field and impact with the cathode surface, liberating atoms.

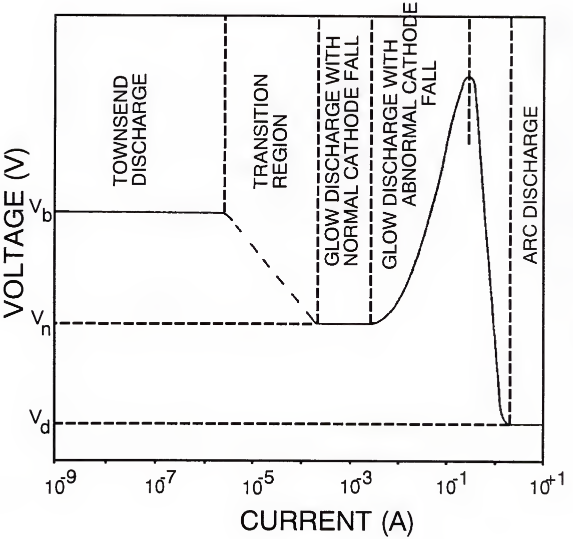

Fig. 2- Relationship between voltage and current in gaseous discharges. (3)

The current at which the discharge is self-sustaining is called the breakdown point. The Townsend discharge is called a "dark discharge" because the electron density is insufficient to create a glow between the electrodes.[36] Increasing the current of about 1 μA transforms the Townsend discharge into a glow discharge. At this point, the voltage and current are high enough to form a characteristic glow. The positive ions multiply until a charge avalanche occurs at a point called the breakdown voltage, when the gas behaves as a partial conductor and the discharge becomes self-sustaining.[36]

A fraction of the argon must be ionized in the electric field to form a gaseous discharge. Expressed by Equation 1-1, this process is called electron impact and is an important process in forming a plasma.[37] Electron impact ionization occurs when a sputtered neutral atom, M°, collides with an electron such that

$$M^{\circ} + e^{-} \rightarrow M^{+} + 2e^{-} \tag{1-1}$$

to form a positive ion, M^{+}.

This process is especially important for the excitation of sputtered analyte. Upon collisions with electrons, an atom can be promoted to higher transition levels, allowing it to be probed by optical spectroscopy. When an excited species relaxes to the ground state it emits photons with energy equal to the specific energy of excitation.[38]

In Figure 2, the glow discharge is divided into normal and abnormal discharges. Normal glow discharges exhibit currents that increase without corresponding increases in voltage, because the current may rise as the plasma enlarges to interact with the entire cathode surface.[38] After the cathode surface is in total contact with the discharge, a further rise in current will result in an increase in voltage and the GD becomes abnormal.

The voltage and current in an abnormal discharge increase electron density until the plasma becomes conducting. There is a loss of resistance and an arc forms between the electrodes, dropping the voltage and terminating the discharge. The high current heats the cathode and can thermally ablate atoms. Because the plasma extinguishes, the arc is termed a non-self-sustaining discharge.

Glow Discharges

This dissertation centers on abnormal glow discharges. These discharges are created by applying a negative potential (-300 to -2000 V) between two electrodes inside a vacuum chamber filled with an inert gas at low pressure (typically 1 Torr). The anode is at ground potential and a negative voltage is applied to the cathode. The potential difference induces a flow of current that interacts with the fill gas and creates ions. Typically, several bright and dark regions are formed between the electrodes. Figure 3 illustrates these different layers of emission. They are characterized by four general regions-the cathode fall, the negative glow, the positive column, and the anode fall. The positive column is absent in glow discharges used for analytical purposes, because the cathode is so much smaller than the anode.

The electric field created by applying a negative voltage to the cathode is not distributed homogeneously between the electrodes but confined to the dark space.[39] A profile of this field is shown in Figure 4. There is a large potential drop at the boundary between the dark space and the negative glow and this is the point where the rate of electrons exiting the dark space is equal to the rate ions entering it. The length of the dark space depends primarily on the pressure of the discharge gas. Higher pressures intensify the interactions between atoms and electrons. Subsequently, the number of ions entering the dark space increases at higher pressures and the length of the dark space reduces.[38] Little emission occurs in the dark space because electrons have a small cross-section for interaction with atoms at high velocities.[39]

Internally, the plasma works toward equilibrium by redistributing its ions and electrons. To balance the flux of ions and electrons, ions must enter the dark space at a velocity higher than provided for by random motion in the field-free negative glow.[17,40] The negative glow is not a homogeneous body of positive and negative charges, but it is instead a neutral mixture of interacting charged and uncharged species.

Visually, the negative glow is a bright cloud which envelopes the cathode. The emission is the result of excited discharge gas atoms that have relaxed spontaneously after collisions with electrons. The primary color of the glow is dependent on the discharge gas. Argon appears blue and neon discharges are red. The discharge color can also be altered by atoms that have come from the cathode or by gaseous impurities. For example, sputtered copper atoms will

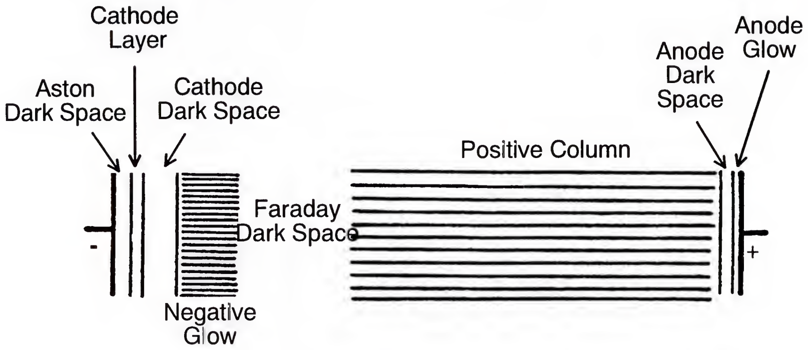

Fig. 3- Luminous zones within a glow discharge tube.

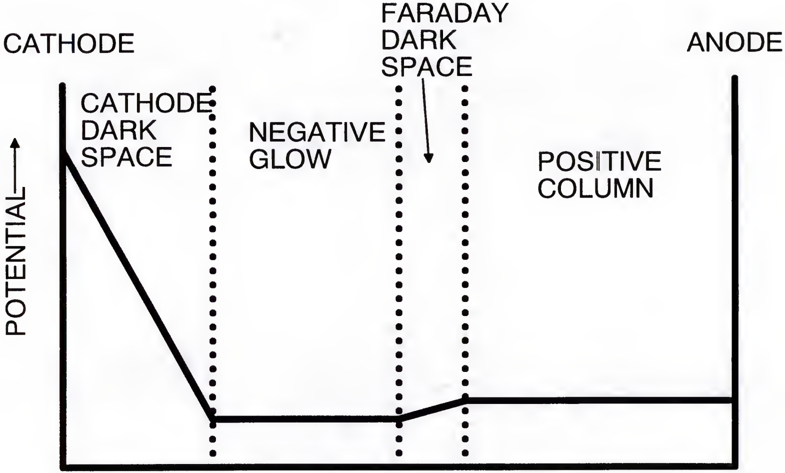

Fig. 4- Potential drop across a glow discharge tube

introduce a green tinge to the negative glow, while water vapor will turn an argon plasma purple.

Plasma Initiation

A GD requires a high voltage between two electrodes immersed in a gas, most often argon. The applied potential causes the atoms and molecules of the gas to break down electrically, and the gas undergoes the transition from being a poor electrical conductor, with a resistivity of $10^{14}\ \Omega\ m^{-1}$, to a good conductor,[41] with a resistivity of approximately $10^{3}\ \Omega\ m^{-1}$.

The electrons are accelerated from the cathode surface through the cathode dark space and into cathode fall. Here, the electrons have accumulated sufficient energy to cause charge multiplication when they strike gaseous species, producing an efficient supply of electrons and ions. The potential difference between the electrodes at which this transition occurs is called the breakdown potential and depends on the identity and pressure of the gas, the electrode material and inter-electrode separation.[42]

The breakdown of the gas results in the formation of positively and negatively charged ions and electrons. Electric fields develop between the electrodes so that positively charged species travel toward the cathode (-) and negatively charged species are accelerated toward the anode (+). Since collisional processes within the discharge produce more charged species, the discharge becomes self-sustaining and continues at a potential lower than the breakdown voltage.[29]

Current flow through a gas demands that the electrons and ion flux be the same. However, electrons are more-mobile than ions. If the negative glow was truly at ground potential, the electron current into it would exceed the arrival rate of ions at the cathode. So the plasma takes on a large positive voltage and the negative glow acts as a vast potential that delays the loss of electrons.

Electron impact ionization occurs when an atom collides with an electron whose energy is higher than the ionization energy of the atom. There are two principal sources of electrons in the negative glow: primary electrons from the cathode surface and secondary electrons which are by-products of ionization by primary electrons.[43]

Most of the electrons in the negative glow are secondary and ultimate electrons. Secondary electrons have varying energies, depending on what is available after the impact which released them from an ion. Ultimate electrons are also secondary electrons which have lost most of their energy through inelastic collisions. Both ultimate and secondary electrons have a Maxwell-Boltzmann energy distribution.[17] Because ultimate electrons are low in energy (less than 1 eV), they cannot cause ionization.[3,44] The mean energy of secondary electrons is around 4 eV.[45] They are large contributors for electron ionization in the negative glow. However, only primary electrons are energetic enough to ionize an inert gas, such as argon.

Once an argon atom is ionized, it begins to move toward the cathode. Its progress may be impeded by collisions with other atoms, ions or electrons.

Whether this occurs depends on a statistical parameter known as the mean free path (λ). The mean free path is the average distance an atom or ion travels before encountering another atom and is given by the equation:

$$\lambda = \frac{1}{\pi n_o \sigma} \tag{1-2}$$

where σ is the collisional cross-section of the colliding atoms and (n_0) is the number density at a given pressure. An atom sweeps out a volume of space based on its velocity and radius as it moves through the gas. Other atoms can be assumed to be distributed evenly within this volume. For argon, σ is assumed to be the square of twice its radius. At 1 Torr, the mean free path is calculated as 0.0076 cm. Taking the mean velocity of argon atoms within the dark space to be 6.6×10^4 cm s^{-1} and a dark space length of 5 mm, argon undergoes about 100 collisions before it strikes the cathode surface.[17] These collisions can slow the ion considerably and result in translational heating of the plasma.

Because the length of the cathode dark space is larger than the mean free paths of the ions and they may undergo multiple collisions as they are accelerated toward the cathode surface, the bombarding ions have various angles of incidence and a wide energy spread.[46]

Sputtering

Positive ions in the negative glow are accelerated across the cathode dark space and impinge the cathode. Ion bombardment energies typically range from 100 to 500 eV.[47] An ion striking the cathode surface either reflects from a surface atom or penetrates the solid, transferring its energy to surface atoms. Depending on its energy and impact angle, the incoming atom transfers its momentum and kinetic energy to the solid target. If the transferred energy is greater than the target's binding energy, the bombardment will release the surface atoms into the gas phase.[48] The transfer of momentum between the incident ion and cathode matrix occurs through a collisional cascade resulting in numerous inelastic and elastic collisions.[3] Figure 5 is a diagram of what happens when the Ar^+ strikes the surface.

When an ion strikes the surface of a solid, it becomes imbedded into the sample matrix and its kinetic energy is taken-up by atoms in the immediate vicinity. As the energy becomes distributed into the sample, it causes a rearrangement of the solid lattice structure.[49] When enough energy is transferred to atoms near the surface, so that their energies are greater than the surface binding energy, the atoms can escape the cathode and enter the gas phase. The minimum energy required to cause this is called the sputtering threshold.[46] At this energy, the ion is said to sputter many atoms from the sample surface. Once free of the sample, a sputtered atom can diffuse into the plasma or redeposit.

The ejected atoms usually originate from only in the first few angstroms of the sample and have energies of 5 to 15 eV.[47] If the sputtered species is ejected as a positive ion, it will be attracted to the negative cathode surface and redeposit.[11] Therefore, over 90% of the sputtered particles that make it into the plasma are ground state, neutral atoms with only a small fraction of ions and molecules being

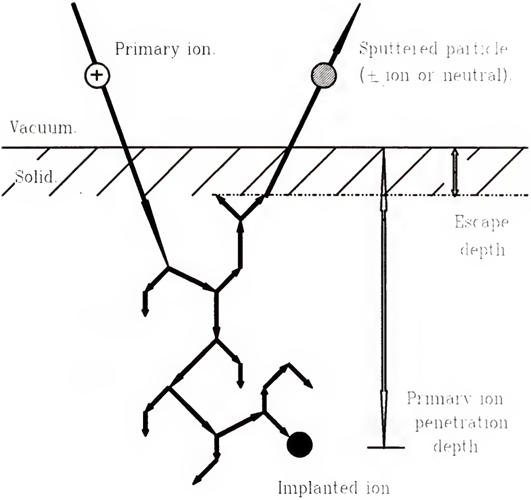

Fig. 5- Process by which incident ions sputter surface atoms.

ejected.[50] Its high atomic population makes the GD a good source for atomic spectroscopy, such as fluorescence and atomic absorption techniques.[7,51]

Sputtering is an inefficient process with more than 95% of the bombarding energy converted to sample heating.[46] The efficiency of a sputtering process can be defined as the sputter yield, S, which is a measure of the number of sputtered atoms per incident ion. The sputter yield can be found by:

$$S=\frac{10^{-6}\ WN\,e}{Mi^{+}t} \qquad (1\text{-}3)$$

where W is the weight loss of the sample (μg), N is Avogadro's number (mol^{-1}), e is the electronic charge (A s), M is the atomic mass (g mol^{-1}) of the sputtered atom, i^+ is the ion current (A), and t is the sputtering time (s).[13]

Besides equation 1-3, the sputter yield is dependent on several other factors, such as the nature of sputter gas, the bombarding angle, the energy of the incident ion, and the type of cathode used.[46,52] A sputter yield study with argon has shown it to have superior sputtering qualities as compared to other inert gases.[53]

The voltage applied to the cathode increases along with the bombarding energies and the sputter yield artificially increases as the temperature approaches the melting point of the metal. This is due to thermal emission of the target material that occurs together with the sputtering process. If higher sputter yields are needed by increasing the bombarding energy, the cathode should be externally cooled.

Often, impurities either on, inside the cathode, or in the fill gas, can reduce the sputter rate. A "dirty" sample may require some time to strip the impurities from the surface, and therefore analyte sample sputtering may not begin immediately upon turning on the discharge. The time to clean the cathode depends on the sample material, the purity of the discharge gas, and the impurities present. Water is a common impurity in the glow discharge. It fragments into many species which are interferents in optical and mass spectra.[54] When water was intentionally added to the GD, a decrease in sputter rate was observed that was dependent on the cathode material.[55]

Sputtering yields vary little from element to element. As shown in Figure 6, the yields typically differ by a factor of 3 to 5.[56] In comparison, elemental thermal volatilities can vary by 4 to 5 orders of magnitude.[57] On this basis, GD atom reservoirs are less prone to effects stemming from matrix variations than are atomization methods which rely on thermal vaporization.

Uneven sputtering rates of different elements may give some cause for concern, because preferential sputtering seems to make it difficult to obtain atom populations in the gas phase proportional to their bulk concentrations.[58,59] However, the glow discharge corrects for preferential sputtering in alloys because the enrichment of the surface with species having smaller sputter yields eventually leads to a reestablishment of equilibrium. After an initial "equalizing" period, the gas phase atomic population becomes proportional to that of the solid sample.[60]

Small molecules can be sputtered into the discharge. Oechsner and

Gerhard observed copper clusters being sputtered from a copper target.[61] They state that molecular sputtering was caused by the aggregation of two or more atoms ejected from one binary collision cascade in the target.[62]

Excitation

After species from the sample cathode arrive in the plasma, they can be promoted to higher energy levels. Figure 7 depicts the negative glow region as a collision-rich environment, where atoms are excited and ionized. These collisions are not only necessary to maintain the GD, but crucial to the analytical potential of the discharge.[63]

The negative glow is considered the most important region in terms of analytical applications. Electron number densities are roughly 10^{11} to 10^{13} cm^{-3}; and electron impact is the primary mechanism for ionization.[64] Between 0.1 and 1% of the plasma population is ionized in this way.[61,65] Furthermore, excited atoms can undergo collisions with electrons and be ionized by the way of cumulative ionization.[66]

Sometimes an electron/atom collision is not completely inelastic and the atom is not ionized, but excited to a higher transition level. This is the case for most collisions with secondary electrons. Via these less energetic interactions, an indirect route for ionization has been found.

Sometimes an atom becomes excited to an energy level from which it cannot radiatively relax, but must decay collisionally. These forbidden energy states are known as metastables.[67] Without a radiative decay pathway to allow spontaneous relaxation of the atom, metastable atoms must rely on inelastic collisions that allow these excited atoms to relax by transferring their energy to a collision partner. This implies that metastable atoms are a medium of stored energy to be released upon collision. F. M. Penning was the first to propose that an atom could be ionized if it interacted with another atom which was trapped in a metastable level.[68] This mechanism is called Penning ionization and is a significant process for excitation in the glow discharge. Possible interactions for metastables are summarized in Figure 1.

Discharge gas atoms undergo electron impact collisions, resulting in the production of metastable gas atoms.[69] These metastables often have energies greater than the first ionization potentials of neutral species. Argon has, for example, metastable energy states of 11.55 eV and 11.72 eV. Metastables are efficiently produced in a glow discharge and have reported densities around 10^{10} to 10^{11} cm^{-3} with the total density of Ar atoms being near 10^{16} cm^{-3}.[22,70] These metastable species can collide with neutral atoms causing ionization. As much as 95% of the overall ionization may occur by the way of Penning mechanism.[71]

Although Penning ionization was proposed in the 1920s, its significance to excitation in the glow discharge was not given attention until its importance was proved by Coburn and Kay.[22,72] Recently, experiments were conducted using a laser and quenching agents to depopulate the Ar metastable atoms to study the induced effect on Penning ionization.[53,73]

Table 1. Ionization and excitation processes in the negative glow region of a glow discharge.

I. Primary Ionization and Excitation Processes

A. Electron Impact

$M^{\circ} + e^{-} \rightarrow M^{+} + 2\,e^{-}$

$M^{\circ} + e^{-} \rightarrow M^{*} + e^{-}$

B. Penning Collisions

$M^{\circ} + A_m^{*} \rightarrow M^{+} + A^{\circ} + e^{-}$

$M^{\circ} + A_m^{*} \rightarrow M^{*} + A^{\circ}$

II. Secondary Processes

A.1. Nonsymmetric Charge Transfer

$M^{\circ} + A^{+} \rightarrow M^{+} + A^{\circ}$

$M^{\circ} + A^{+} \rightarrow M^{+*} + A^{\circ}$

2. Symmetric (Resonance) Charge Transfer

$X^{+}_{(fast)} + X^{\circ}_{(slow)} \rightarrow X^{\circ}_{(fast)} + X^{+}_{(slow)}$

3. Dissociative Charge Transfer

$MX + A^{+} \rightarrow M^{+} + X + A^{\circ}$

B. Associative Ionization

$M + A_m^{*} \rightarrow MA^{+} + e^{-}$

C. Photoionization and excitation

$M^{\circ} + h\nu \rightarrow M^{+} + e^{-}$

$M^{\circ} + h\nu \rightarrow M^{*}$

D. Cumulative Ionization

$M^{\circ} + e^{-} \rightarrow M^{*} + e^{-} \rightarrow M^{+} + 2e^{-}$

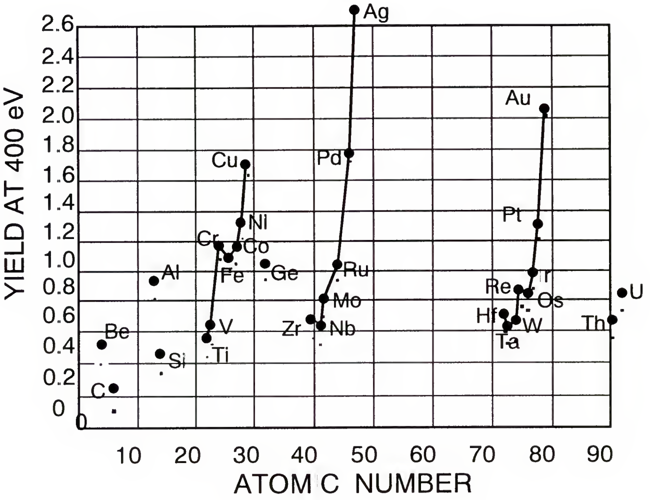

Fig. 6- Sputter yields for various elements. (63)

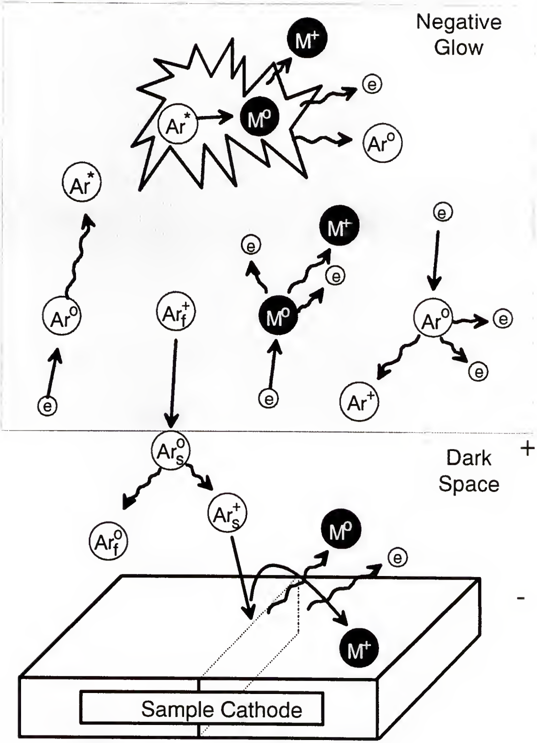

Fig. 7- Gas phase reactions in the negative glow.

For the work in this dissertation, atomic excitation by metastables is a more important process. Electron promotion to atomic levels requires less energy transfer and accounts for most of the emission observed in the plasma. The lifetimes of metastable atoms are on the order of milliseconds, in contrast to electronic relaxation that occurs within 1 ns.[74] Because metastable atoms rely on collisional deexcitation, pressure is a factor influencing the lifetime of the metastable state. Discharge pressures above 1 Torr result in shorter metastable lifetimes, since collisions occur more frequently.[75]

According to Delcroix *et al.,* the number density of metastable atoms (n_m) is related to the number density of electrons (n_e), the neutral species number density (n_0), a coefficient for the production rate of metastables (C_p), and the rate at which metastable atoms are lost (Y).[76] At low current densities and constant pressure, a linear relationship exists between n_m and n_e, such that

$$n_m = n_e n_0 C_p \,/\, Y. \tag{1-4}$$

An upper limit is reached for metastable formation as destruction by electron impact becomes competitive.

Metastable populations can also be affected by the presence of impurities, which reduce the total ionization rate due to energy consumption by the excitation of molecular vibrations.[77] Water vapor and organic molecules have been observed to quench metastable populations by absorbing energy.[78]

Modes of Operation

The major difference between a RF and a DC discharge is that the RF discharge is oscillating between a positive and negative voltage while the DC maintains a steady negative voltage.

Direct current discharges

The DC discharge is the most commonly used glow discharge type in spectroscopy. One reason for this popularity is the ease with which a DC discharge can be created using a conducting sample. The discharge housing serves as the grounded anode, and a negative voltage is applied to the sample. A positive voltage would cause the discharge housing to sputter instead of the sample.

The DC discharge can be operated in either the constant voltage or constant current mode. With constant voltage, the power supply is held at a fixed potential between the cathode and anode, supplying whatever current necessary to maintain that voltage. This method controls the energy with which ions strike the sample surface, but the total number of ions will vary with the discharge's resistance, which varies with many parameters such as with the pressure. In contrast, with constant current, the total number of ions arriving at the cathode per second is controlled, but their impact energy will vary as the power supply adjusts the applied voltage to maintain the specified current for changing conditions. Some power supplies allow the total power to be set constant, at the expense of the independent control of current and voltage.

Radio frequency discharges

The RF glow discharge is more complicated than its DC counterpart, both in theory of operation and application to the analysis of solid samples. One important reason to consider the RF glow discharge as an atomization source is its ability to sputter both conducting and nonconducting samples. When a high power, alternating current is applied to a nonconducting sample, the cathode potential drops to a negative value and decays with time to a more positive potential as the bombarding ions neutralize the cathode surface. This is because a nonconducting sample in a RF discharge behaves like a capacitor as the sample surface alternates between negative and positive potentials.

Pulsed Glow Discharges

History

Pulsed glow discharges are good emission sources and exhibit higher reproducibility than DC sources.[79] They have been used as sources for atomic spectroscopy and mass spectrometry. Winefordner *et al.* have used laser excited fluorescence in the dark period between pulses to measure atomic populations in the discharge.[80] When the power is interrupted, emission signals dissipate rapidly while the sputtered atoms require a longer time to diffuse from the plasma.[12] This method has the advantage of eliminating background emission for fluorescence spectra; detection limits in the femtogram range for some elements have been reported.[80]

The most notable application of pulsed techniques is to improve the output of hollow cathode lamps for use in fluorescence and atomic absorption work.[81] Dawson showed a greater than 50 fold increase in the output intensity of pulsed discharge lamps versus continuously operating lamps.[82] Using five different lamps as fluorescence excitation sources, pulsed GD lamps have been used for the simultaneous multielement analysis of nebulized samples.[14] These lamps were sequentially pulsed, producing short bursts of resonant radiation that selectively excited elements in a flame.

Pulsing either DC or RF glow discharge sources also produces increased ion signals.[20,83] Pulsed discharges exhibit a factor of two higher ion signals than DC discharges. When observing different regions of the pulse period, some ion signal anomalies were found that allowed discrimination against certain interfering species.[84,85]

Pulse Characteristics

In a pulsed glow discharge, the applied voltage is interrupted to periodically extinguish the discharge. Pulsing of the discharge creates time-dependent signals that have been useful for both fundamental studies and analytical applications.

At the beginning of the pulse cycle, the distinguishing feature is an increase in the ion and emission signals for contaminant gas species, called the "prepeak." This initiation period of the pulsed discharge is controlled by the rapidly changing energy of electrons emitted from the sample surface. The plateau region results once the pulsed discharge reaches a steady state. Steady state conditions are disturbed again at the termination of the discharge pulse, causing a spike in the analyte signal, the "afterpeak."

The prepeak

The prepeak region occurs from the beginning of the discharge pulse to the time that ion signals reach a plateau value. The prepeak is evident in a mass spectral profile for the contaminant gas species, H_2O^+, in Figure 8b. It should also be noted that only gaseous species (Ar^+, H_2O^+, N_2^+) have prepeaks and they appear prior to the signals of sputtered species. The pathway is presumed to be by electron impact, since these gaseous species cannot be effectively excited by metastables.[3]

The prepeak is absent in the ion and emission profiles for sputtered species. Instead, the sputtered species signal gradually increases to a plateau value. Both sputtered and contaminant gas signals reach a plateau value as the applied voltage stabilizes and remains unchanged for the remainder the pulse period, regardless of the pulse duration.

The intensity of the prepeak is related to the plateau and associated with the applied voltage. As the voltage is reduced, the prepeak disappears. This is due to primary electron energies that are too low to transfer their energy to molecules in the negative glow.[85]

The plateau

After the sputtered population infiltrates the negative glow, it may also undergo electron impact. Since these atoms thermalize a certain number of electron themselves, the number of gas species being excited decreases to a steady-state value.[78] Once the pulsed discharge reaches the plateau, there is little change in signal intensities until the plasma terminates. For contaminant gases, the plateau is reached some 3 ms into the pulse period, after the prepeak decays. Sputtered species require the same time to reach their plateau value, including the time it takes for them to arrive into the plasma.

At the termination of the applied voltage, the signals for sputtered species and contaminant gases again behave differently. Gas signals rapidly decay to the baseline at the end of the pulse, while the sputtered species signal intensity increases at the end of the pulse and forms an afterpeak.

The afterpeak

The most important feature of a pulsed GD is seen after the voltage is terminated, when a surge in ion and emission signals occurs, called the afterpeak. This is seen for copper in Figure 8c. In an argon discharge, only species with ionization energies below the energy levels of argon metastable atoms exhibit afterpeaks. This points to the conclusion that Penning excitation is the principal ionization mechanism after termination of the discharge. The role of Penning excitation in the afterpeak was investigated by altering selected discharge parameters expected to interfere with metastable ionization of sputtered analyte atoms.

Electron densities in pulsed discharges were measured using a resonant microwave cavity.[86] It was observed that electron populations decrease within 100

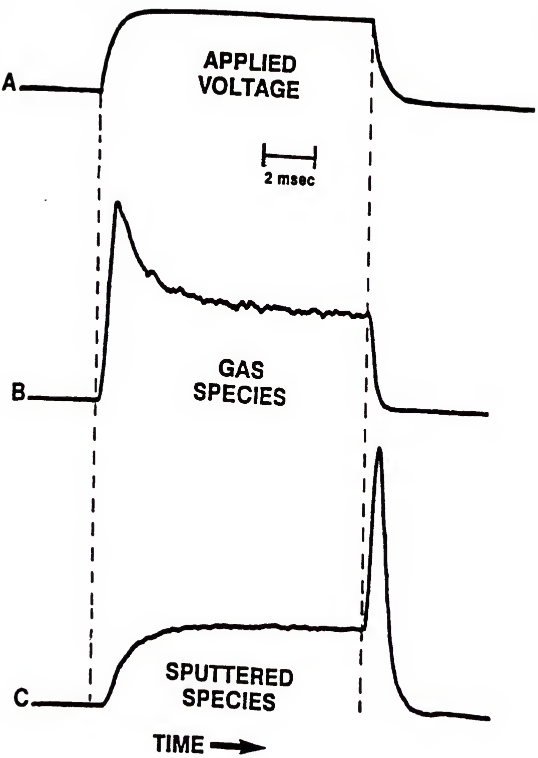

Fig. 8- Profiles for millisecond-pulsed glow discharge. (83)

µs after the voltage is turned off. Using atomic absorption spectroscopy, Strauss *et al.* monitored the metastable population in the post-pulse region and observed it to increase within the first few hundred microseconds after the discharge was terminated.[87] Barshick conducted a time-resolved atomic absorption study in the afterpeak region using an argon discharge with copper.[58] Metastable population remained constant for 150 µs following the collapse of the discharge. Similar results were obtained when a resistively heated filament was used to inject electrons into the discharge, indicating the intensity of the afterpeak is inversely proportional to the flux of electrons from the filament.[53] The presence of electrons in the post-pulse period reduces the intensity of the afterpeak, presumably by deexciting the metastable atoms.

The population of argon metastable atoms in the glow discharge is a balance of their formation and destruction.[88] When the voltage is terminated, primary electrons are no longer available and the population of electrons energetic enough to ionize the gas species declines. Since the production of thermalized electrons in the afterpeak ceases, the principal source of metastable atoms is eliminated. On the other hand, primary electrons also deexcite metastable atoms. Without energetic electrons, metastable atoms rely on other collisional processes to relax, such as energy transfer.[87] Because the reduction in primary electron number density and because the collisional cross section for metastable atoms are an order of magnitude higher than electrons, analyte signals after the voltage shuts off and the afterpeak appears.[89]

CHAPTER 2
ATOMIC FLUORESCENCE SPECTROSCOPY

History

At the turn of the century, Wood observed that sodium vapor will radiate its own light when exposed to radiation from a very intense sodium flame.[90, 91] He named this effect resonance radiation, and it has come to be known as fluorescence. Atomic fluorescence is actually emission, in which the excitation step involves the absorption of a photon, with the energy of a specific electron transition level for an element, and a subsequent de-excitation that produces a secondary photon.

In the early 1920's, the use of atomic fluorescence spectroscopy (AFS) for chemical analysis began when a flame was employed as the atom cell to simultaneously detect thallium, calcium, barium, strontium, lithium, and sodium.[92] The next advance in AFS came from Boers *et al.* who used this technique as a diagnostic tool to find physical information concerning elements and atom reservoirs.[93] AFS provided data on fundamental mechanisms, such as the lifetimes of excited states and transition coefficients, which are valuable for optimizing other analytical techniques.[94]

During the early days of AFS, there were few uses of this technique for the analysis of real samples, and there were already other popular methods that could be used, such as atomic emission (AES) or atomic absorption spectroscopy (AAS). Consequently, fluorescence techniques were confined mainly to fundamental research.

In 1964, Winefordner and Vickers[32] used a metal vapor discharge tube as the excitation source for zinc, mercury, cadmium, and thallium in an oxygen/acetylene flame; they reported detection limits on the order of 1 ppm. After further improvements, detection limits were obtained that established AFS as a rival to AES and AAS in sensitivity.[95,96]

AFS has been applied to biological samples including urine[97] and blood.[98] In these matrices mercury, cadmium and other metals were detected at concentrations as low as 5 ng/ml. Other applications that have been found for AFS are in metallurgy,[99,100] environmental analyses[101] and fuel component determinations.[102] Background interference due to the scattering of incident radiation is a common problem encountered with AFS, and at high atom concentrations self-absorption can produce a nonlinear response. However, atomic fluorescence techniques do enjoy unprecedented sensitivity and selectivity along with a linear dynamic range of up to seven orders of magnitude.[103]

Sometimes the analyte matrix can affect fluorescence signals severely by collisionally de-exciting the excited state, called quenching, or by binding to the element of interest. This "matrix effect" is the main problem affecting most analytical methods and can become severe even for atomic emission, atomic absorption, and mass spectrometric techniques. For fluorescence, the main limitation is a lack of "ideal" excitation sources that limits its commercial viability.

Theory

Flames and tungsten lamps are continuum sources and were the first external light sources used to excite atomic fluorescence. Tungsten lamps are broadband sources, emitting a wide continuum of wavelengths. Flames emit a series of lines, depending on what elements they contain. Both sources can induce fluorescence for many elements at once. The major drawback of a continuum source is that it generally produces a small flux of photons over a particular atomic bandwidth as compared with line sources. Thus, continuum sources are unable to saturate atomic transitions for most elements, which is necessary for trace analysis. However, the more recently developed high pressure xenon lamps offer the highest output of all continuum sources. Nonetheless, for a single wavelength they can not compare to most line sources, such as electrodeless discharge lamps (EDL), hollow cathode lamps (HCL), and lasers.

Soon after a direct relationship between the fluorescence signal and analyte concentration was recognized for a wide range of atomic populations, the sensitivity and selectivity of AFS were further established when lasers were incorporated as excitation sources.[104,105] The picometer resolution capabilities of these intense sources enhance the inherent selectivity of atomic fluorescence.[106-108]

The exact relationship of an analyte signal to the concentration of an analyte can be shown through the derivation of the fluorescence flux expression. This mathematical treatment is outlined by Winefordner and Epstein.[109] They use a simple two-level atom system under resonance fluorescence conditions, such that the excitation wavelength and emission wavelength are identical. A representation of this atomic transition is shown in Figure 9. Examining the possible excitation and de-excitation processes involved in resonance fluorescence allows a general understanding of fluorescence theory.

Usually, the rate equation approach is a valid way to address LEAFS theory and it has been outlined in the literature[110] and the approach given here is based on this discussion. This treatment begins by approximating the populations of a two level atomic system (Figure 9) with the lower level (i) representing the ground state, and the upper level (j) being the excited state of this atomic system. The population densities, n_i and n_j, for these two levels can be described in terms of radiative and nonradiative rates of excitation and de-excitation processes, which add to or deplete the population of the desired level, respectively. Some assumptions made for a rate model are that the atoms are in a dilute, gaseous phase at atmospheric pressure, and there are no external fields present. Their distribution in the energy levels follows the Boltzmann distribution

$$\frac{n_j}{n_i} = \frac{g_j}{g_i} \exp\left(-\frac{h\nu}{kT}\right) \tag{2-1}$$

where h is Planck's constant (J·s), v is the frequency of the transition between levels i and j, k is the Boltzmann constant (J/K), g_i and g_j are the degeneracies of levels i and j, respectively, n_i and n_j are the population densities of levels i and j

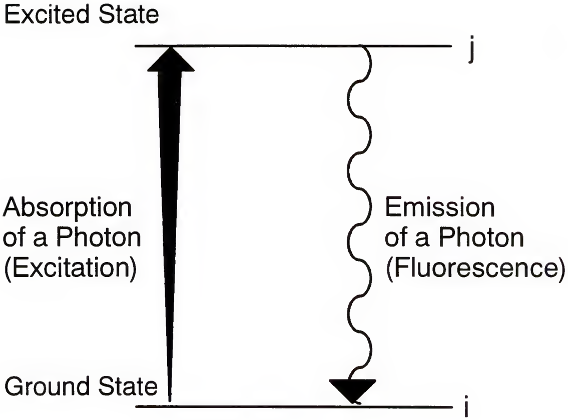

Fig. 9- A two level system for fluorescence.

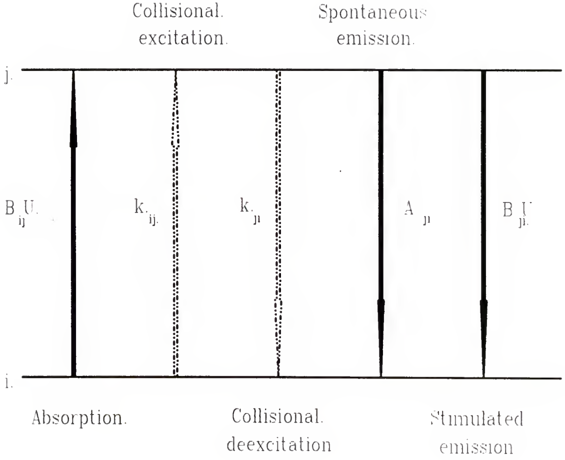

Fig. 10- Pathways for excitation and de-excitation in a two level system

(atoms/cm^3), respectively, and T is the temperature of the system (K). A diagram showing the different pathways through which these two levels can be populated is shown in Figure 10. The rate equation depicting the decay of atoms from level j, neglecting collisional contributions, is given as

$$\frac{dn_j}{dt} = -n_j A_{ji} \qquad (2\text{-}2)$$

where A_{ji} is the Einstein coefficient of spontaneous emission from the excited state to the ground state (s^{-1}).

The time dependent relationship depicting the changes in the population density of the excited level is written as the sum of the forward and reverse rate equations. Once the atoms are excited to the upper level, two primary processes are responsible for their return to the ground state, emission of a photon and collisions. We can quantify the fluorescence power yield, Y, as the fraction of absorbed radiant power emitted at some wavelength. The radiant power is the flux (photons s^{-1}) multiplied by the photon energy, for a resonance transition. The quantum yield is given as

$$Y = \frac{A_{ji}}{A_{ji} + k_{ji}} \qquad (2\text{-}3)$$

where k_{ji} is the rate constant for collisional de-excitation (s^{-1}).[111,112]

The efficiency of the fluorescence process is related to atomic parameters. The total fluorescence power produced, Φ_F, in the volume element V by absorption

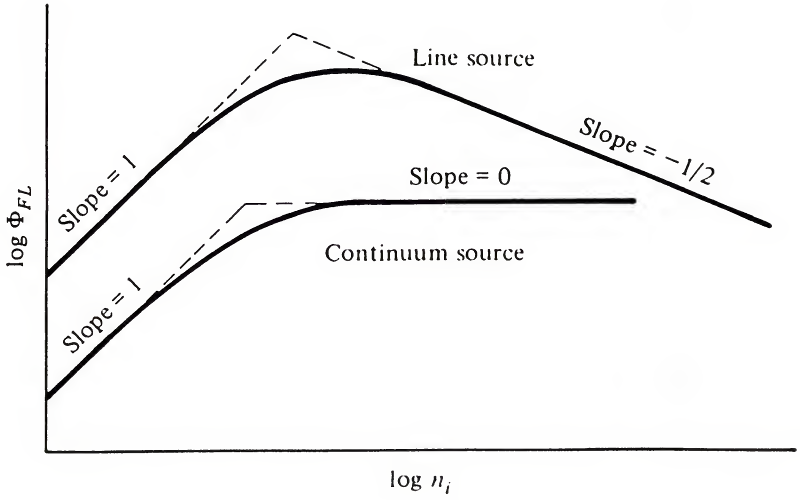

Fig. 11- Fluorescence curves for continuum and line sources. (34)

over pathlength l is given by

$$\Phi_F = \Phi_o \alpha_L Y \tag{2-4}$$

where Φ_o is the incident source radiant power (J s^{-1}), and α_L is the absorption factor for a line source.[34]

$$\alpha_L = 1 - e^{-k_m l} \tag{2-5}$$

This absorption factor under optically thin conditions can be reduced to

$$\alpha_L = k_m l \tag{2-6}$$

where l is the pathlength (m), and k_m is the maximum absorption coefficient (m^{-1}) and can be expressed as

$$k_m = \frac{e^2 \lambda_m^2 n_i f_{ij}}{4 \varepsilon_o m_e c^2 \Delta \lambda_{eff}} \tag{2-7}$$

where e is the electron charge (C), λ_m is the wavelength of the transition (m), f_{ij} is the absorption oscillator strength (dimensionless), ε_o is the permittivity of free space (J^{-1} C^2 m^{-1}), m_e is the electron mass (kg), c is the speed of light (m s^{-1}), and $\Delta\lambda_{eff}$ is the effective width of the absorption line (m).[110]

After substituting equations (2-7) and (2-6) into (2-4) and evaluating constants, the total fluorescence power produced can be written as:

$$\Phi_F = \frac{8.82 \times 10^{-13}\ \lambda_m^2 n_i f_{ij} l \Phi_o Y}{\Delta\lambda_{eff}} \tag{2-8}$$

where the constant has units of meters. Hence, the observed radiant power of fluorescence is directly proportional to the number density of the ground state. This relationship is the basis of AFS.

Nonlinear effects

When probing a high atomic population with atomic fluorescence, some nonlinear effects can be expected. The absorption factor as expressed in equation (2-4) approaches unity:

$$\Phi_F = \Phi_o Y. \tag{2-9}$$

The fluorescence signal becomes independent of the atomic population in the ground state. Self-absorption also becomes a factor at high atomic concentrations. The observed fluorescence radiant power (J s^{-1} m^{-1}), Φ_F', is then given by:

$$\Phi_F' = \Phi_F f_s \tag{2-10}$$

where f_s is the fraction of fluorescent photons not reabsorbed; it is unity at low concentrations.[109] Atomic fluorescence is only linearly related to the analyte concentration at low concentrations; at high atomic densities the self absorption factor becomes:

$$f_s=2\sqrt{\frac{a}{k_m l\pi.}} \qquad (2\text{-}11)$$

Therefore, upon increasing the atomic population, eventually the LEAFS signal decreases proportionally to ($n^{-1/2}$). Curves that relate number density to signal for both continuum and line sources are given in Figure 11.

Although self-absorption is the major cause of nonlinearity at high analyte concentrations, two other phenomena may also play a role. These effects, termed pre-filter and post-filter effects, are related to the right angle fluorescence detection geometry that is frequently used. [111,112] In this configuration, the fluorescence is observed at 90° from the path of the radiation beam. The source radiation may be reduced before it reaches the analytical region, or the fluorescence produced can be absorbed before it reaches the detector by the cooler, ground state atoms in these areas. The cell may not be completely illuminated by the source and the fluorescence is incompletely measured, if the source light is attenuated in front of the analytical region. This is the pre-filter effect which leads to bending of the calibration graphs at lower concentrations. The post-filter effect involves the adequate illumination of the analytical volume, but the fluorescence intensity is reduced due to the re-absorption of fluorescence by atoms that are outside this volume in the direction of the detector. This effect may decrease the linear dynamic range by orders of magnitude.

The performance characteristics of LEAFS are exceptional, but no commercial instruments are available mainly due to the associated unreliability, complexity and high cost of lasers.[110,113] The continuum source has advantages in these respects, while also allowing simultaneous multielement detection. Fluorescence offers a larger linear dynamic range and better precision and accuracy than atomic absorption and atomic emission along with low limits of detection. However, the detection limits and precision are often limited by the atomizer through its efficiency and associated noise.[112]

Atomic Reservoirs

When considering an atom source for AFS, there are several desirable parameters to consider.[34] The ideal reservoir would have an atomization efficiency of unity with all of the analyte being converted to an atomic vapor. The atomizer should cause minimal thermal excitation of emission from the analyte and other species present in the sample. Furthermore, the environment should be such that the fluorescence quantum efficiency is maximized and be free from colliding species that could cause the fluorescence to be quenched. An inert atmosphere is also ideal to minimize compound formation. Many atom sources have been routinely utilized in LEAFS, including most often flames, inductively coupled plasmas (ICPs), graphite furnace electrothermal atomizers and, more infrequently, low pressure discharges or GDs.[110,111] Each atom reservoir has certain advantages and disadvantages.

Flames are simple to use, but are associated with high background emission that can be a substantial source of noise. Inert gases can be premixed with the combustion gases to reduce quenching with a subsequent reduction in atomization efficiency. Additionally, the excitation radiation can be scattered by particles in the flame, adding further to the noise level.

The ICP has a high excitation efficiency and a large continuum background, thus the power, temperature and observation region must be carefully optimized.[34] Using graphite furnaces as the atomic reservoir for fluorescence is a promising analytical technique, because electrothermal atomizers have several advantages. The discrete analysis of samples in the microliter range is possible, resulting in low absolute detection limits; in contrast ICP and flame sources require milliliters of sample. The atomization time is extremely short and a high instantaneous number density is obtained. An inert atmosphere can again be employed to reduce quenching. There are problems, however, with analyte interferences, blackbody emission and background absorption by molecular species regarding the graphite furnace.

The GD has been described as the ideal atom reservoir mainly because atoms are produced non-thermally through sputtering.[3] As a result, these plasmas are less prone to effects arising from matrix variations, because this low pressure, inert gas environment is a reduced quenching environment. Disadvantages associated with these sources include poor precision and atomization efficiency. Nevertheless, this source is an excellent choice as an atomizer for fluorescence, and single atom detection with GD-LEAFS seems possible.[114,115] A schematic of GD-LEAFS which achieved an L.O.D for lead of 8 pg[116] is given in Figure 12.

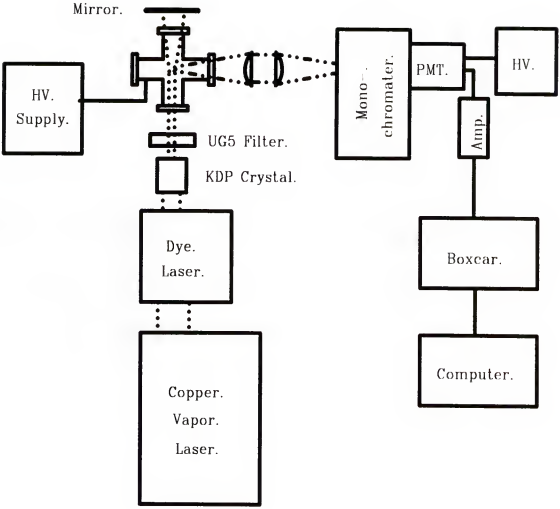

Fig. 12- Schematic of the GD-LEAFS experimental system. (115)

CHAPTER 3
MULTIELEMENT GLOW DISCHARGE ATOMIC FLUORESCENCE

Introduction

Glow discharge atomic fluorescence (GDAFS) using continuum sources has been studied as a sampling technique for solids. Our work has concentrated on evaluating multielement GDAFS for base metal analysis as an alternative to glow discharge atomic emission (GDAES), and glow discharge mass spectrometry (GDMS).

The GD is the chosen atom source for these experiments. Previously, it has been established to be a good atom source for atomic emission especially with respect to its ease in analyzing solid samples. However, there are many characteristics of the GD that also suggests it is an excellent atom source for atomic fluorescence. Cathodic sputtering produces a large atomic population directly into the gas phase and these atoms exist primarily in their ground state, due to the low power of the GD plasma. This high atomic ground state population is sputtered into an inert atmosphere, ~1 torr argon, and is not subject to collisional de-excitation and pressure broadening that occurs in atmospheric sources, like flames, ETVs and ICPs.

Previous fluorescence methods employing the glow discharge as an atom reservoir have used line sources for excitation. For example, tunable lasers allow for selective, single element detection with excellent limits of detection.[117] In contrast to using an expensive and complex dye-laser as an excitation source for atomic fluorescence, we have used a spectral continuum xenon arc lamp and a xenon flashlamp. These are sufficiently intense continuum excitation sources to promote atomic fluorescence within the GD plasma. Continuum source atomic fluorescence has been discussed in detail by Butcher *et al.*[110]

Xenon lamps are conventional, broadband light sources with many advantageous features for atomic fluorescence spectrometry. Figure 13 shows a typical emission spectrum of a high pressure xenon flashlamp. Xenon lamps spread their total energy between a wide spectral range and their emission intensity output over an atomic bandwidth is smaller than compared to a dye laser. Consequently, atomic fluorescence is more difficult to saturate with them. It is more urgent to tightly focus the emission of these lamps onto the analytical atomic volume and accurately image the resulting fluorescence onto the detector (monochromator). The main problem is that conventional source radiation, unlike laser radiation, is isotropic and must be collimated and focused by lenses. High collimation reduces the output intensity of the lamp, along with the potential fluorescence signal that can be observed. However, little collimation allows an excessive amount of diverging light to enter the GD cell, increasing the background scatter noise incident on the detector. Therefore, the amount of prefocusing of the excitation beam is critical in maximizing the signal-to-noise ratio.

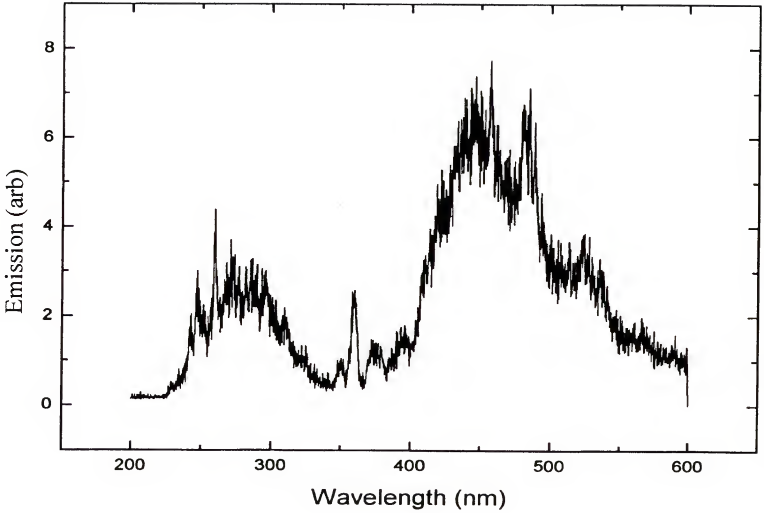

Fig. 13- Xenon flashlamp emission spectrum.

GDAES and glow discharge atomic absorption spectrometry (GDAAS) have long been used as analytical methods and as diagnostic techniques in studies of plasma chemistry.[118] The more widely used GDAES, a multielement technique, exhibits inherent problems with spectral interferences. These arise mainly from the complex emission spectra of the fill gas and/or the emission spectra of the molecular impurities present in the discharge (e.g., N_2, H_20, etc).[5] Our objective is to produce spectra free of both the sputter gas and molecular emission lines. Xenon lamps readily excite metallic species but cannot promote noble gases to their high, first level excited states. A fluorescence spectrum is relatively free from background fluorescence because the fill gas, argon, has its resonance transitions below 200 nm. Molecular impurities such as N_2 generally have much lower oscillator strengths than those of atomic species, making molecular fluorescence weak in comparison. Therefore, atomic fluorescence spectra are expected to be substantially less complex than emission spectra. It is on this principle that metal species can be detected by fluorescence without a complicated emission pattern of the sputter gas that might obscure the analyte's signal.

Broadband xenon arc lamps and flashlamps have smaller source radiances over an atomic excitation bandwidth as compared to many line sources. By its manual, the Eimac 300 W xenon arc lamp has a spectral irradiance of 0.1 mW/nm at 300 nm. While typical dye lasers output around 1000 W/nm. However, the xenon lamps have the capability of exciting atomic fluorescence within many atomic reservoirs, including ICP's,[119] graphite furnaces,[120] and flames.[121] These studies involved the analyses of trace metal species in aqueous solutions, wherein detection limits of 200 ppb magnesium in a water sample were observed using the graphite furnace along with a 150 W xenon arc lamp. These lamps show greater stability, allow for greater reproducibility, and have longer lifetime than line sources. More importantly, the xenon arc lamp produces a nearly constant output over a wide spectral range, which is preferred for rapid multielement analysis.

The observed fluorescence spectra appear relatively free of both the argon fill gas emission lines and molecular impurity lines that often obscure trace metal detection in GDAES. Additionally, the low energy GD plasma leaves a majority of its atoms in the ground state or a low lying electronic state, resulting in a much simpler metal fluorescence spectrum than generally observed with more energetic atomic reservoirs.

Experimental

Traditionally, the glow discharge has been operated using either a DC or RF power supply. When a DC power supply is used, the sample must be electrically conducting such as a metal alloy. If the sample is a nonconducting powder, it can be mixed with a conducting powder and pressed into a suitable cathode shape. In this work, a high voltage programmable DC power supply (Model OPS-3500, Kepco, Flushing NY, USA) powered the discharge, and the discharge was normally operated in the pulsed mode (25 Hz) when using the xenon flashlamp.

A copper sample holder fits on the end of a direct insertion probe (DIP), which is a coaxial cathode feedthrough that allows the convenient exchange of samples for the analysis of solids and solutions.[122] The DIP has a single feedthrough with a shaft 1/2 inch in diameter and is placed in the discharge chamber by passing it through a Cajon® high-vacuum fitting. With this probe the cathode sample can be moved vertically within the glow discharge to optimize the signal-to-background ratio for the highest atomic population and lowest background emission from the negative glow.

A nonconducting machinable ceramic [Macor, Corning Glass Works, Corning, NY] shield was placed over the copper holder to isolate the glow discharge plasma to the sample surface. Macor® was used because it can be fabricated into a variety of shapes, has good insulating properties, and is easily cleaned by sandblasting. Figure 14 is a schematic diagram of the typical arrangement of shielding, sample holder, and cathode mounting used with samples that are cut into pin shapes. To delay arcing due to the shield being fouled with redeposition products from the sample, the Macor should cover the mounting hardware without touching the cathode. If the space between the shield and the cathode is wider than the length of the dark space, a discharge can form behind the shield.[3]

The glow discharge's operating conditions of pressure, current, and voltage was optimized for peak fluorescence with each sample and mode of power delivery. The formation of excited state species or atoms can be favored in the glow discharge plasma by varying the discharge operating parameters. The pressure was monitored in the range of 0 - 20 millimeters Hg using an analogue gauge (Thermocouple gauge DV-4D,Teledyne Hastings-Raydist, Hasting, VA, USA).

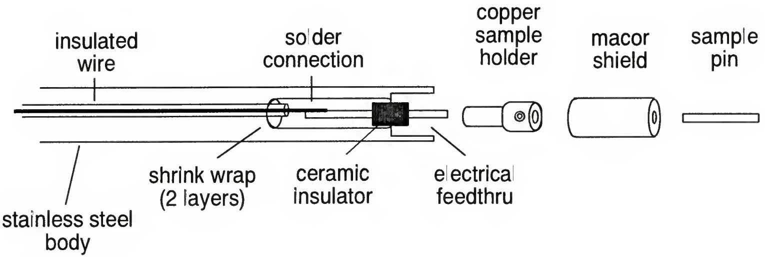

Fig. 14- Exploded view of the direct insertion probe and cathode assembly

The ceramic sleeve isolates sputtering to the probe tip, allowing 5 mm of the 2 mm diameter cathode pin to be exposed. When a 5 mm diameter disk was used, only the surface was exposed to the discharge. Ultra high purity argon (99.995% pure, Alfagaz, Walnut Creek, CA, USA) was used as the sputter gas. Quartz lenses were used for all windows to allow the transmission of UV radiation.

The schematic diagram shown in Figure 15 is generalized for both xenon sources. The axes of the sample pin, the excitation beam, and the fluorescence column viewed by the monochromator are perpendicular to each other. This geometry reduces scatter off the cathode from reaching the detector, along with the strong emission that occurs near the cathode surface.

The 300 W xenon arc lamp (ILC Technology, Sunnyvale CA, USA, Cermax) was operated continuously and always at its maximum output power. The DC output of the arc lamp allows the use of a chopper. The chopper was synchronized to a lock-in amplifier (Model 186A, EG&G Applied Research, Salem MA, USA), which also receives signals from the monochromator's PMT. The lock-in discriminates fluorescence from emission by subtracting the emission of the GD when the chopper blocks the arc lamp, from the concurrent fluorescence and emission detected when the arc lamp is focused into the GD cell.

A scanning monochromator (EU-700, GCA/McPherson, Acton, MA, USA) having a grating with a blaze wavelength of 250 nm was employed. The grating has a groove density of 1180 grv/mm and a reciprocal linear dispersion of 1.8 nm/mm. The glow discharge was imaged 1:1 on the entrance slit using a 68 mm diameter

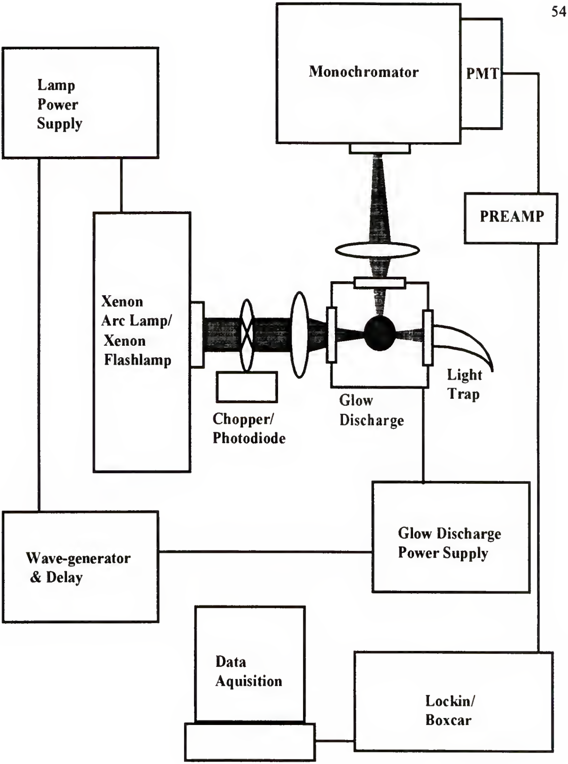

Fig. 15- Schematic for multielement GDAFS using xenon lamps

quartz biconvex lens with a 50 mm focal length. Spatially resolved measurements of the glow discharge were taken by moving the lens perpendicular to the optical axis, or by moving the probe. The entrance and exit slit widths were usually 50 µm and the entrance slit height was 10 mm. A photomultiplier tube (Model R955, Hamamatsu, Bridgewater, NJ, USA) produced an output current that was converted to a voltage by a small transimpedance amplifier (Model A-1, Thorn EMI, Rockaway, NJ, US A). The output current was recorded using a strip chart recorder (Houston Instruments, Austin, TX, USA). In the alternative setup, a xenon flashlamp (Model 457A, Xenon Corp, Woburn, MA, USA) emits a short (2 µs), intense (1 MW) pulse to excite atomic fluorescence which was detected with a photomultiplier tube coupled to a gated boxcar (Model 250, Stanford Research Systems, Sunnyvale CA, USA); a photodiode was used to trigger the boxcar gate. The photodiode trigger signal was sent to the data system at the beginning of the pulse cycle. The timing between the pulsed discharge and the boxcar was controlled by a pulse delay box that can slow the arrival of the trigger pulse up to 20 ms. The usual procedure is to initiate the pulsed discharge and using one channel of an oscilloscope to observe the resulting emission at a particular wavelength. The gate from the signal processor was simultaneously displayed on the second oscilloscope channel. The position of the data gate was adjusted while observing their position relative to the pulsed emission signal. This procedure allows a data gate as narrow as 500 ns to be placed anywhere in the pulse period. The signal processor will integrate the total number of counts collected for the duration of the data gate and then pass this information to the computer. In this way, all spectra were digitized and sent to a computer for processing by an A/D converter (Model 245, Stanford Research Systems, Sunnyvale CA, USA).

The steel six way cross was originally made for a mass spectrometer. The quartz windows for the inlet and exit windows on the original setup were about 3 inches from the cathode at the center. This distance minimizes sputter deposition on these windows, but reduces the light throughput and signal. With this cell configuration, it becomes necessary to use a long focal length lens (4 inches) to concentrate the flashlamp's light onto the analytical region viewed by the monochromator. A shorter focal length lens is better able to reduce the beam waist and increase to flux of photons available for the initial excitation. The GD's entrance window arm had been reduced to a distance of 1.5 inches from the cathode, so that a 2 inch focal length lens could be used to focus the excitation beam. The argon gas inlet was split into three streams and entered the GD directly behind the entrance window facing the flashlamp. This way of introducing the fill gas serves to shield the window from sputter deposition by forming a deflecting high pressure region in front of the window. The opposing exit window, an escape for unused lamp radiation, was replaced by a Wood's horn light trap, eliminating potential backscattering of radiation which increased upon allowing sputter deposition to compound on an exit window.

Xenon Arc Lamp

Initially, the 300 W continuous wave (cw) xenon arc lamp was employed to excite atomic fluorescence within the glow discharge. A lock-in amplifier was used to discriminate fluorescence from the constant emission of the plasma. The cw arc lamp was found to only excite strong, resonance, ground state atomic fluorescence lines of the sputtered metal species.

A pure copper cathode was first to be evaluated as shown in the spectra in Figure 16b. Copper's strongest lines are 324.7 and 327.4 nm; these were the only lines observed in fluorescence spectra using the xenon arc lamp. Emission spectra from the glow discharge are much more complex than fluorescence spectra, with many spectral lines originating not only from many excited states of sputtered analyte species, but also from the argon fill gas and molecular concomitants. Figure 16a shows some of these interferences as broad molecular bands along with a multitude of argon emission lines. The two intense copper lines (324.7 and 327.4 nm) are clearly apparent as major constituents of the plasma.

It can be seen that both molecular bands and many more atomic lines appearing in the emission spectrum are missing in the fluorescence spectrum obtained by use of a xenon arc lamp. The only significant spectral interferant observed in the fluorescence spectrum is a weak OH fluorescence band at 306 nm. In comparing the two spectra, it should be noted that the relative intensities of the two copper lines are reversed in the fluorescence spectra. According to the reported transition probabilities the 324.7 nm line should be about 50% more intense than the companion resonance line at 327.4 nm, a ratio accurately reflected in the GD emission spectrum. In the GD fluorescence spectrum, the 324.7 nm i

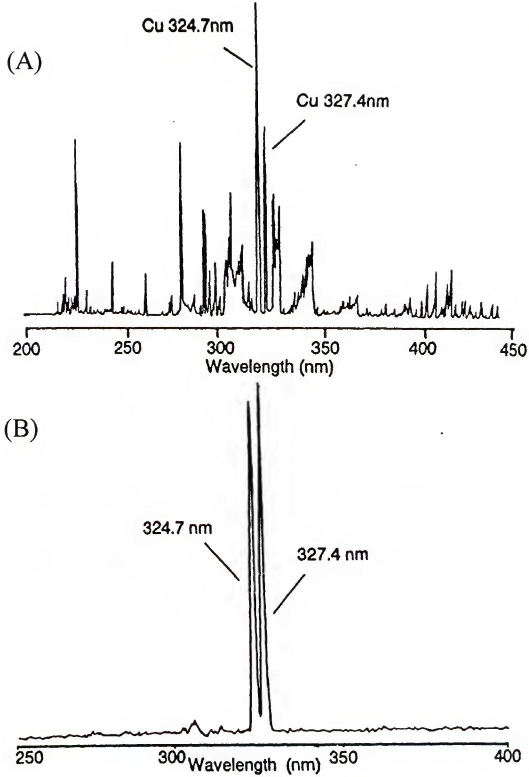

Fig. 16- Glow discharge spectra. A) Emission. B) Fluorescence.

intensity is consistently the smaller of the two, caused by greater self absorption for the 324.7 nm line. The GD conditions are chosen for the highest fluorescence signal-to-background ratios and fluorescence signals generally increase with increased sputtering.

Fluorescence lines appear with intensities about 1/2 than of the same lines observed in emission spectra. However, the strong and numerous background emission lines of argon can easily interfere with analytical lines in the UV region. Argon emission is not seen in fluorescence spectra because of efficient lock-in subtraction. More importantly, argon's first excited states require photon energies much higher than that produced by the arc lamp (~100 nm).

Argon atoms are less abundant at relatively low pressures, 0.1 torr, and which reduces sputter yields. However, at higher pressures lower sputter yields are obtained due to a higher contribution of redeposition.[78] The fluorescence signal-to-background is optimum at 1.1 torr in argon (Figure 17). All fluorescence spectra were taken at this pressure. Also, sputtering yields, and therefore fluorescence signals, were found to increase in direct proportion with current. The maximum current allowed to pass through the GD at a particular pressure is limited by voltage. The current supplied at 1.1 torr and 1000 V is limited to 2 mA. These are the ideal conditions used for obtaining spectra with the xenon arc lamp. On the other hand, excited state species become more abundant with increasing pressure, until the GD reaches very high pressures, >5 torr, when the collisional cross sections of electrons and argon atoms increase resulting in lower energy electrons and a smaller ionized argon population.[3] The emission output is a convolution of sputter yield and the collisional excitation rate of the electrons, which reaches a maximum when these two parameters are compromised. The optimum conditions for emission are found to be 1.9 torr, 1500 V, and 3.8 mA; these are the conditions set for all subsequent emission spectra.

In Figure 18, it is observed that when moving nearer to the cathode sample, both the atomic ground state population (fluorescence) and the excited state population (emission) increase. However, scattering off of the cathode or the inside of the chamber can easily overwhelm the signal and become the limiting noise.

Xenon Flashlamp

The arc lamp, because of its weak emission output, was abandoned for the more intense xenon flashlamp. The flashlamp outputs a 2 µs pulse of light at 6 kV and can be operated up to 30 Hz. The major fundamental problem that dominates when using the arc lamp to excite fluorescence the low intensity output over all atomic line bandwidth. After slight modifications to the GD and replacing the arc lamp with the xenon flashlamp excitation source, the signal-to-background was substantially increased indicating the possible use of the xenon flashlamp for multielement GDAFS. This is achieved through both a reduction in background scatter and an increase in signal intensity. The xenon flashlamp emits a pulse of continuum light which is nearly 5000 times more intense than the xenon arc lamp during the on-time. A boxcar is used to measure the fluorescence signal along with

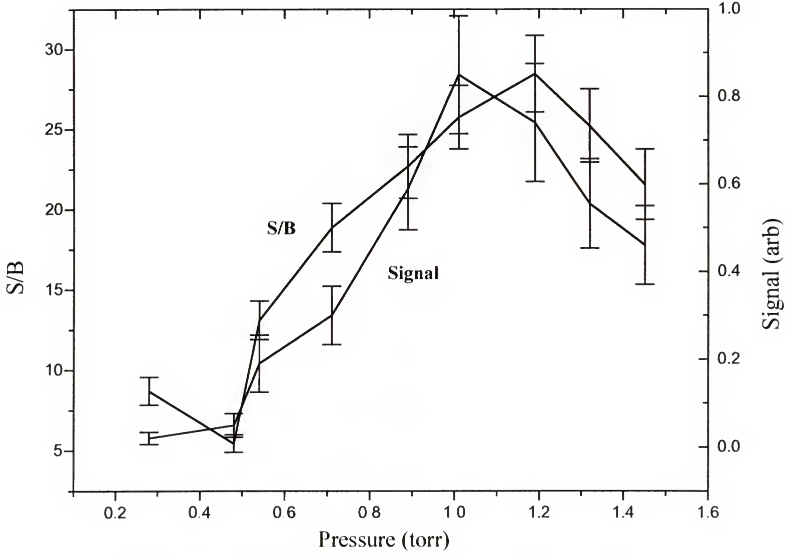

Fig. 17- Signal and S/B for the Cu 324.7 nm line vs GD Pressure, 3.8% in aluminum.

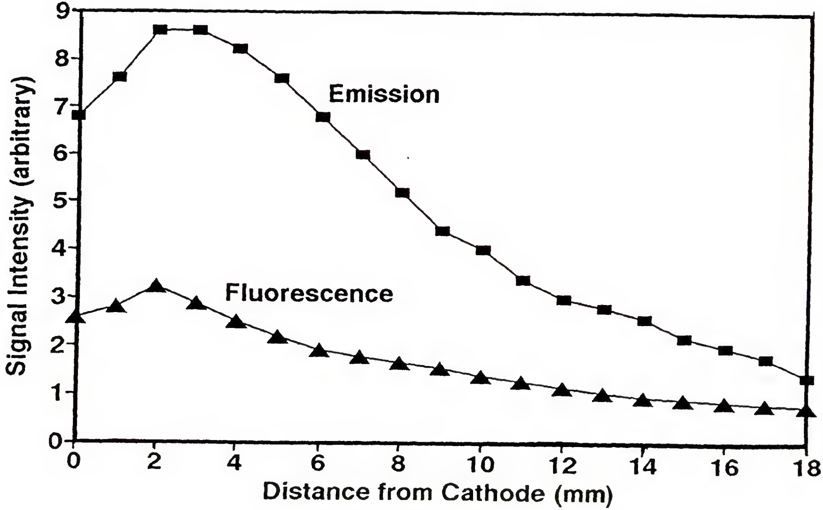

Fig. 18- Spatial profile of emission and fluorescence signals.

any DC emission collected during the short gate width.

A flashlamp source has an additional advantage in combination with the pulsed mode of the glow discharge.[85] Turning off the discharge causes the plasma to collapse; emission can be discriminated against by synchronously pulsing the GD and firing the flashlamp at some desired delay after the discharge is switched off. By operating the glow discharge in a pulsed configuration, the temporal zone immediately after glow discharge termination can be used advantageously; during this period, a substantial sputtered atom population remains after the undesired background emission has declined to near zero. The flashlamp can be triggered to fire at some optimum delay time after discharge termination, resulting in a large reduction in background emission during the measurement interval.

The prolonged decay of fluorescence indicates an atomic diffusion rate much slower than the de-excitation rate of excited atoms to the ground state. Comparisons of the emission and fluorescence spectra demonstrate the improvement in signal to background of fluorescence over emission with use of the xenon arc lamp. The decay of the atomic population is given by the plot of the signal-to-background in Figure 19, which shows delay intervals of 16 ms. The data in Figure 19 indicates a change in the line intensity ratio with time after discharge termination. The ratio of the two lines inverts twice over the entire pulse width. At first, the 324.7 nm line is larger than the 327.4 nm line, then they reverse in intensity and reach a constant ratio during the plateau region. At 20 ms after the discharge turns off, the ratio obtains the correct value of about 1.8 based upon the ratio of gf values. A closer look at the copper lines during the initiation of the discharge is given in Figure 20. Both the persistence and reversal of the strong copper lines, 324.7 and 327.4 nm, after long flashlamp delays allude to strong self-absorption, thus suggesting large initial atom populations when the discharge is running.

Copper emission and fluorescence spectra at several delay times after termination of the glow discharge are shown. The upper set of emission spectra in Figure 21 (delay = 0) shows a typical GD emission response taken just prior to discharge extinction. Typical line and band features are observed. Successive spectra taken at 2 ms intervals after discharge termination show a rapid drop in intensities of all features because of the prompt removal of electrons, ions, and excited states. However, the lower fluorescence spectra in Figure 21 reveals that strong copper fluorescence spectra can still be obtained 16 ms after the discharge is terminated, suggesting a long lifetime of sputtered atoms available for excitation with the pulsed xenon lamp. Note that the copper peaks at 324.7 nm and 327.4 nm gradually invert in intensity as the atomic population decreases with time, approaching their normally anticipated values.

The flashlamp, by the virtue of its greater intensity, is a much more efficient fluorescence source than the xenon arc lamp and spectra obtained using the xenon flashlamp with the pure copper cathode exhibit higher signal-to-noise ratios than those obtained with the arc lamp. In contrast with the copper fluorescence spectrum obtained from the xenon arc lamp, the xenon flashlamp is able to excite

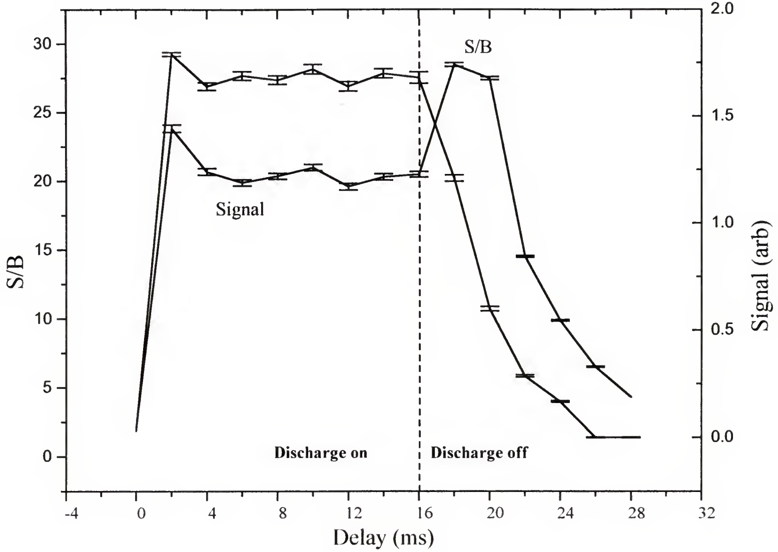

Fig. 19- Cu 249.2 nm Fluorescence profile and S/B for a pulsed GD

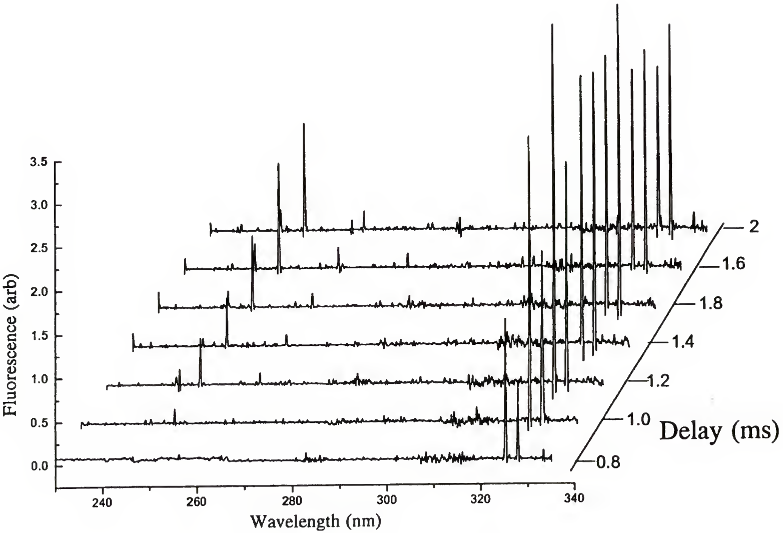

Fig. 20- Fluorescence spectra at the initiation of the pulsed glow discharge.

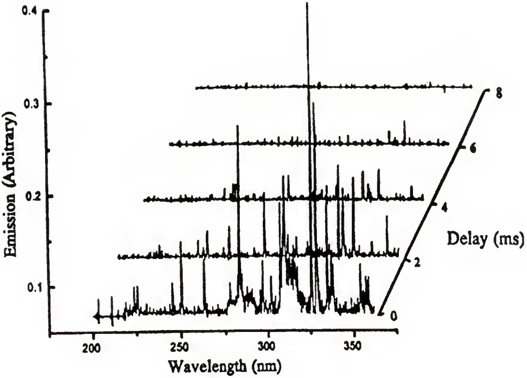

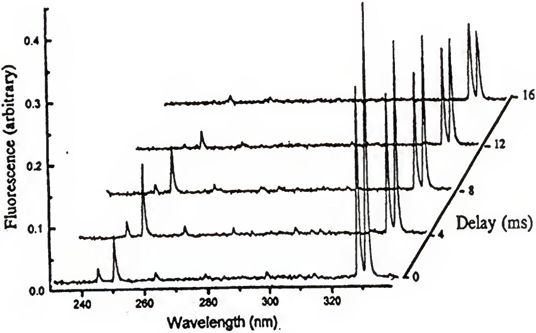

Fig. 21- Temporal spectra observed after the discharge s terminated
Upper plto is emission and lower plot is fluorescence.

many weaker resonance lines of copper. These lines are well resolved in Figure 22, which is a fluorescence spectrum with a pure copper cathode using the xenon flashlamp with a delay of 2 ms. Many weak Cu resonance lines can be observed, with good S/B, along with a Cu metastable line at 261.8 nm. These lines were not observed in the spectra using the arc lamp. Therefore, the flashlamp allows many fundamental studies to be performed not possible with the arc lamp, along with increasing analytical sensitivity.

Glow Discharge Characteristics

In previous studies, the glow discharge was operated in a pulsed mode using a programmable DC power supply.[123,124] It is proposed that a sudden loss of electrons is necessary to result in the afterpeak. The increase in emission signals is associated with long lived metastable atoms, that would normally have been de-excited by electron collisions, surviving long enough to transfer their energy to analyte atoms still randomly moving in the discharge. From fluorescence studies using pulsed discharges, it is known that background emission becomes insignificant in about 1 ms.[125]

When operating pulsed discharges at the same average current as an uninterrupted DC discharge, it is necessary to increase the discharge voltage. As the voltage increases to drive the higher currents over shorter duty cycles, the intensity of the afterpeak increases, along with sputter yields. Besides providing a means to increase the applied voltage, pulsing the GD provides a time for the cathode to cool. This can be important since certain cathode types, such as

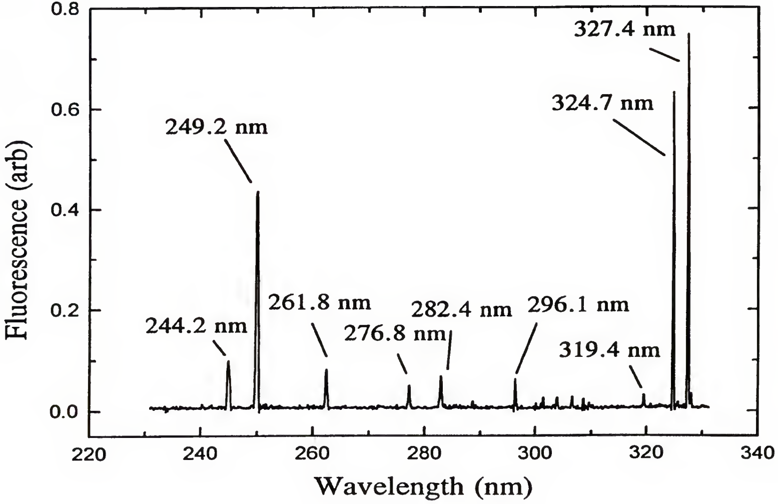

Fig. 22- Copper emission spectrum using the xenon flashlamp

aluminum and zinc, will easily melt at moderate temperatures.

In a steady-state discharge, the sample is continuously sputtered by energetic argon ions that remove the surface layers and maintain a "clean" cathode. In the pulsed discharge, the sputtering process is periodically interrupted, and the sample is exposed to a flux of argon atoms that can adsorb onto the sample surface.[126] At a pressure of 1 torr, the rate at which argon atoms arrive at the surface is approximately 3.5×10^{14} atoms cm^{-2} μs^{-1}.[3] Co-adsorbing with the argon can be contaminant gases such as water, carbon dioxide and nitrogen.

Some of these gases can react with the cathode to form several layers on the surface. This could have a significant influence on the sample surface, especially over long off times, and result in a difficulty in sputtering. Although contaminant gas concentrations are small (0.001%) in the high purity argon used, chemisorption is a cumulative effect.

Diagnostics

The flashlamp produces an intense burst of light with a pulse width of 2 µs. Because atomic fluorescence is virtually instantaneous relative to this time frame, it has become possible to perform some temporal studies on the pulsed GD plasma. The ability to delay the firing of the flashlamp and measure fluorescence in different pulse regions has already been shown useful in analytical applications, particularly for probing the atomic population in dark region after the discharge is extinguished. Alternatively, the flashlamp is capable of profiling the atomic population as it diffuses into the GD chamber.

Everytime the pulsed discharge turns off there is an interruption in atomic sputtering from the cathode surface. At this point, the concentration of free atoms in the discharge is maximized, subsequently decreasing as the atoms diffuse to the walls. The rate of diffusion is called the diffusion lifetime, τ, the time required for a population to drop to 1/e (0.368) of its original concentration. The diffusion lifetime is related to the diffusion coefficient, D, by the following equation.

$$\tau = L^2/(\pi^2 D) \tag{3-1}$$

where L is the diameter of the diffusion chamber (2.5 cm) and the diffusion coefficient can be approximated for a gaseous binary system by the equation

$$D = \frac{3(2\pi k^3 T^3/\mu)^{1/2}}{16 P \pi \sigma^2} \tag{3-2}$$

where μ is the reduced mass (kg), T is the temperature of the gas (K), k is the Boltzmann constant, and σ is the collisional cross section of the colliding species (cm^2).[127] P represents the pressure within the GD (kg/cm·s^2) and is found through the relationship, P=nkT, where n is the number density of the atomic population.

When a pure copper cathode is used, the GD is considered a binary mixture of copper and argon. Calculations yield a diffusion coefficient and diffusion lifetime for copper of 470 cm^2/s and 1.3 ms, respectively. Figure 23 shows a fluorescence decay curve taken for a pure copper cathode at 324.7 nm. The experimental diffusion lifetime remains constant at approximately 2.1 ms although the experimental value is higher than the calculated value of 1.35 ms.

An aluminum sample, NIST #602, was evaluated in a similar way to the copper sample. Figure 24 is the fluorescence decay of the aluminum 309.2 nm line from the point at which the discharge was terminated. The afterpeak lasts 1 ms before the fluorescence is seen to decrease. The experimental diffusion lifetime is 1.2 ms and closely approximates the calculated lifetime for aluminum of 1.3 ms.

The NIST #602 sample contains 1.49% of magnesium which should have a faster diffusion time (1.2 ms) than copper or aluminum due to its smaller collisional cross section. However, as seen in Figure 25, the largest diffusion time found for magnesium is 1.9 ms, which decreases considerably upon moving further into the dark region. This behavior for magnesium is likely to be caused by its increased vapor pressure compared to the other two elements. The number density (n) depends on the vapor pressure P (atm) for a particular element and the temperature (K) of the surrounding gas and it can be calculated by:

$$n = 7.34 x 10^{21} \frac{P}{T} \qquad 3\text{-}3$$

where the vapor pressure is tabulated for an element at a particular gaseous pressure and temperature.[128] Within the glow discharge at 1.5 torr and 600 K, the number densities for aluminum and copper are 2.0 x 10^{-2} atoms/cm^3 and 1.3 x 10^{-4} atoms/cm^3, respectively. On the other hand, magnesium has a number density of 1.9 x 10^{12} atoms/cm^3. Thus, the additional contribution of magnesium atoms to the gas phase due to thermal ablation might be the primary cause for the nonlinear

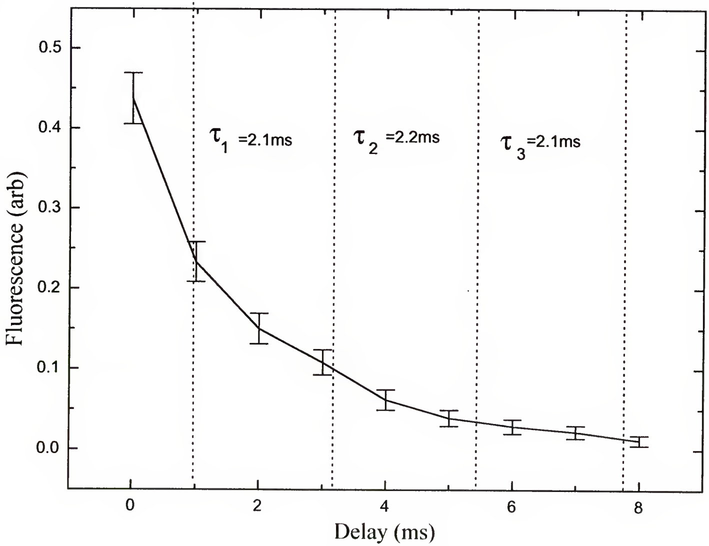

Fig. 23- Cu 324.7 nm fluorescence decay in NIST #602, 1.5 torr, 2.0 watts.

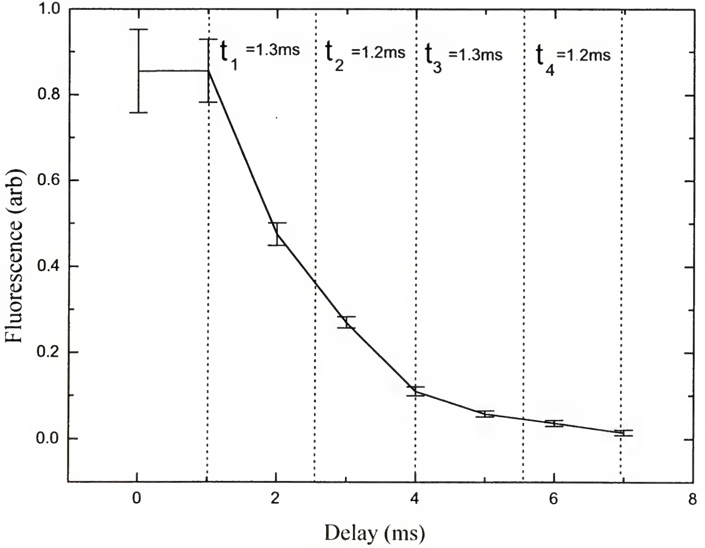

Fig. 24- Decay of Al 309.1nm fluorescence signal, 1.5 torr, 2.0 watts.

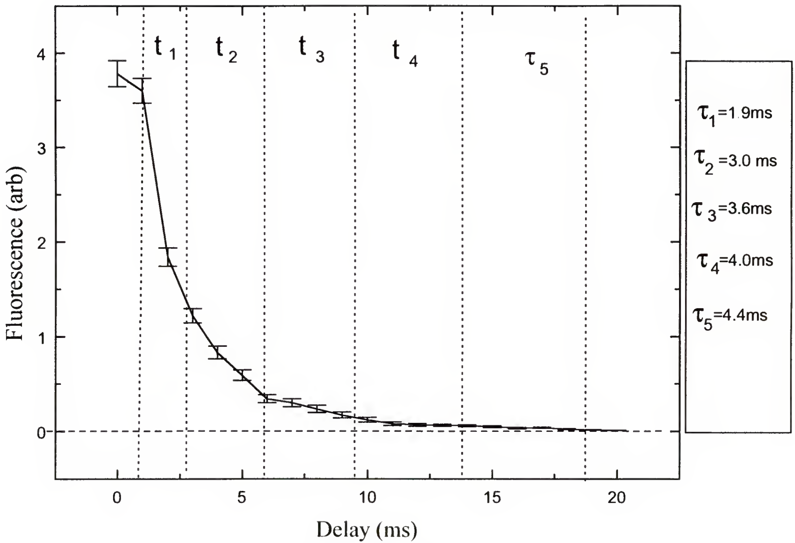

Fig. 25- Decay of Mg 285.2 nm fluorescence signal, 1.5 torr, 2.0 watts.

diffusion lifetime as seen in Figure 25.

Analytical Usefulness

The present GDAFS system has several limitations for elemental analysis, particularly a lower L.O.D. as compared with that can be observed with emission. An attempt was made to determine its potential usefulness using standard reference materials. With both continuous wave and pulsed source lamps, the multielement detection of Al, Mg, Cu, Cr and Mn has been observed from an aluminum sample, NIST SRM #601-604. Figure 26 shows a typical pulsed fluorescence spectrum over a wavelength range which includes spectral lines from Al, Mn, Mg and Cu, obtained with a temporal delay of 3 ms. The spectrum is of SRM #602, which contains 93.43% Al, 4.44% Cu, 1.49% Mg, and 0.63% Mn. The calibration curve for magnesium, Figure 27, is linear and shows the possibility for this method to be used as an inexpensive analytical tool in the rapid identification of metal samples. Glow discharge conditions were maintained constant, at the same values used to obtain Figure 27, throughout the series of measurements, resulting in a linear calibration curve with a regression coefficient of 0.9992.

Limits of detection of tens of ppm were obtained for most elements, although a detection limit of 50 ppm was observed for Mg as measured at 285.2 nm using the xenon flashlamp. L.O.D.'s are obtained by internal precision of 3 sigmas multiplied by the blank noise is determined as the rms noise detected sitting at 322.5 nm, where background emission and fluorescence intensities are low, and divided by the signal found by scanning the line. The large R.S.D. found is due to sampling

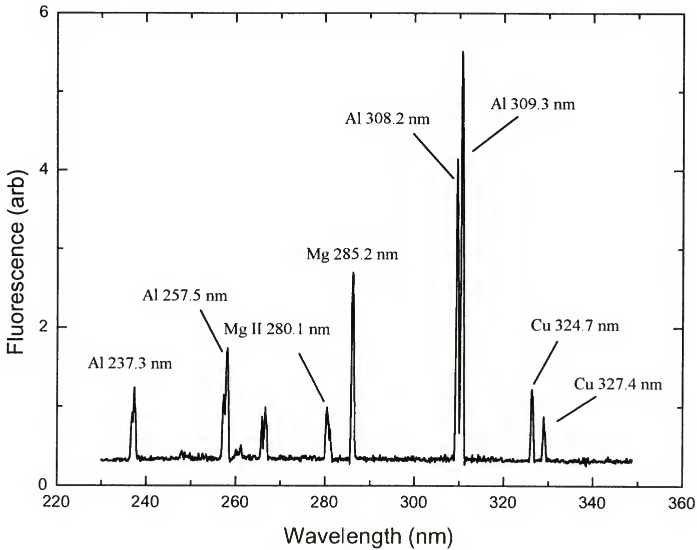

Fig. 26- Aluminum NIST #602 fluorescence spectrum, 3.98% Cu, 1.56% Mg.

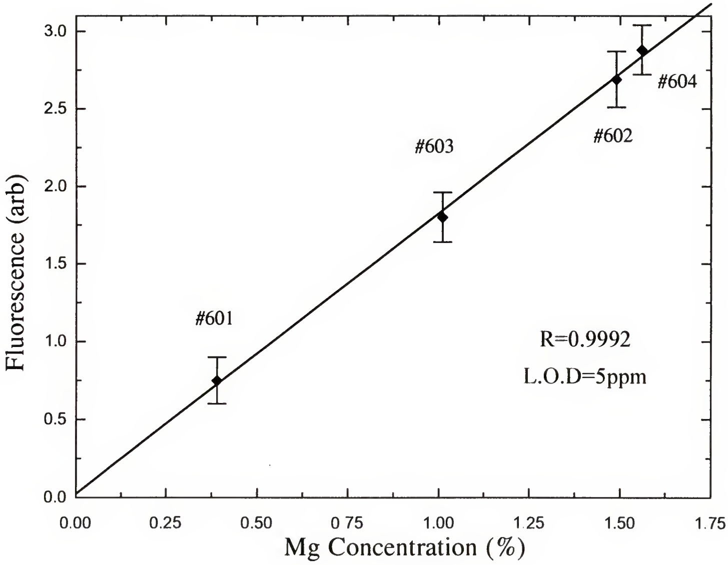

Fig. 27- Calibration curve for magnesium in aluminium

error using three different cathodes of the same type.

Comparison between emission and fluorescence for some of the other materials show the simplicity of fluorescence spectra. The tantalum emission lines in Figure 28 overlap each other and are not baseline resolved; in the fluorescence spectrum fewer lines are excited and they are better resolved. Like tantalum, iron has a great number of atomic transitions. This is seen in Figure 29, which depicts the emission and fluorescence spectra of steel, NIST SRM #462. The iron emission lines obscure many of the trace elements which are found in the steel. For example, manganese is present at 0.94 ppm and the Mn triplet (279.5, 279.8, and 280.1 nm) is seen by fluorescence in Figure 30, but cannot be resolved by emission.

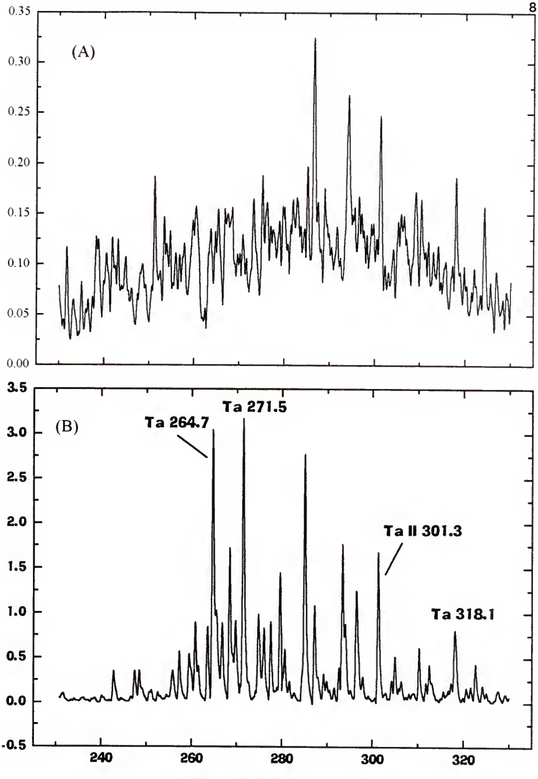

Fig. 28- Tantalum GD spectra. (A) emission (B) fluorescence.

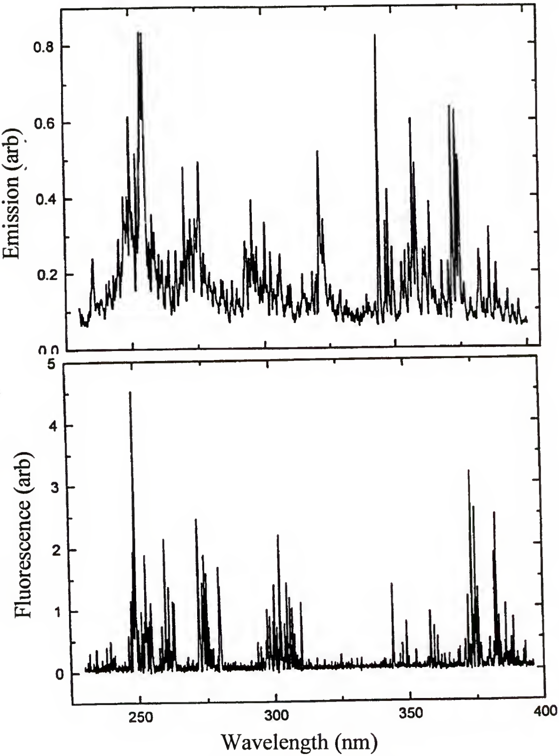

Fig. 29- Steel NIST #462. A) Emission spectrum.B)Fluorescence spectrum

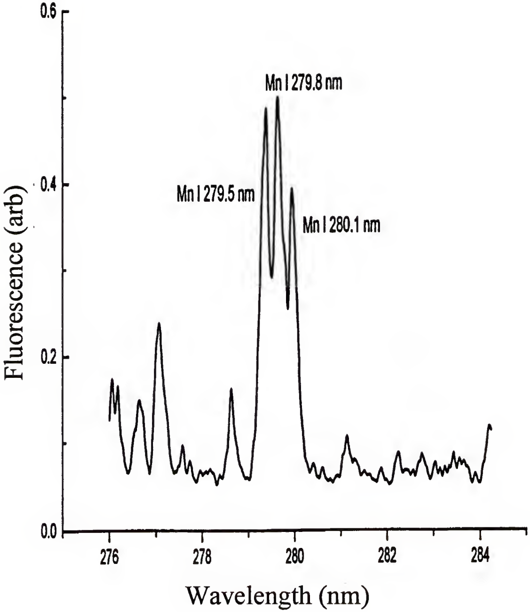

Fig. 30 Manganese fluorescence in steel NIST #462.

CHAPTER 4
THE MICROSECOND PULSED GLOW DISCHARGE

Introduction

The emission from a glow discharge (GD) device was observed almost a century before its widespread acceptance for analytical spectroscopy. Modifications and of applications for the GD have exploded in recent years. Much of the current research has shifted from optical spectroscopy to mass spectrometry (GDMS). This change in focus stems from mass spectrometry's greater sensitivity and lower number of spectral interferences. On the other hand, glow discharge atomic emission spectroscopy (GDAES) remains an attractive alternative to GDMS, due to its simpler instrumentation and lower cost.

Certain modifications in the GD have sparked interest for improving the viability of GDAES as an analytical technique. In previous work, the glow discharge was operated in a pulsed mode using a programmable DC power supply.[129] This pulsed discharge had typical rise times of one millisecond and pulse widths as short as several milliseconds. A rise in emission and ion signals, called the afterpeak, commonly occurs after the plasma is terminated.[130] A few-fold increase in detection limits has been observed by probing the afterpeak emission region of a pulsed glow discharge.

The characteristics of millisecond pulsed glow discharges have been known for many years. These pulsed discharges had typical rise times of one millisecond and pulse widths as short as several milliseconds. Strauss *et al.* attributed the afterpeak to a rise in the argon metastable population from electron recombination due to the collapsing electrical field.[131] The pulsed glow discharge (GD) has also been found useful as a source for fluorescence methods.[132,133] After the plasma is extinguished, the emission decays rapidly while the atomic population diffuses at a slower rate (refer to Chapter 3). This creates a dark period where atomic fluorescence can be probed without being affected by atomic emission.

Originally, the pulsed glow discharge was studied for its ability to produce higher ion currents for glow discharge mass spectrometry. While the overall advantage to the analytical signal was small, other features were observed which led to the use of the pulsed discharge for diagnostic work. Of particular interest was the enhanced ion signal from sputtered species during the collapse of the discharge. Immediately after plasma initiation, about 2 ms required for the discharge to reach equilibration by electron impact.[130] For pulses with halfwidths greater than 5 ms, the discharge has ample time to obtain a steady state voltage (plateau), at which time it operates similarly to a DC discharge. Although by increasing the voltage up to a threefold enhancement in signal compared to DC discharges has been observed, the power applied to the cathode is ultimately limited by the melting temperature of the cathode material.

Since shorter duty cycles allow higher driving voltages and result in larger signals, it would follow that shortening the pulse width and increasing the driving current might induce an even greater signal. This has been verified by several researchers using hollow cathode lamps as sources for atomic absorption; they reported a 10 - 500 times rise in various line intensities.[134,135] Hang *et al.* used a microsecond-pulsed glow discharge (MPGD) to supply a discrete packet of ions for a time-of-flight mass spectrometer.[136] They reported GD pulse widths of only a few microseconds and peak powers on the order of several amperes. In this chapter, I will characterize the MPGD as a good analytical source for solids with emission, and spectroscopically diagnose this unique plasma to gain a further understanding into underlying features of all discharges.

Experimental

A schematic diagram of the apparatus used to characterize microsecond pulsed glow discharge atomic emission spectroscopy (MPGD/AES) is shown in Figure 31. The pin sample was mounted onto the tip of a direct insertion probe. This probe was then inserted into a 6-way cross, which acted as the GD chamber. Perpendicular to the probe was the window port which led to the entrance slit of the monochromator. Opposite the monochromator and perpendicular to the sample, was a hollow cathode lamp used for atomic absorption. For atomic fluorescence studies, a xenon flashlamp (Model 457A,

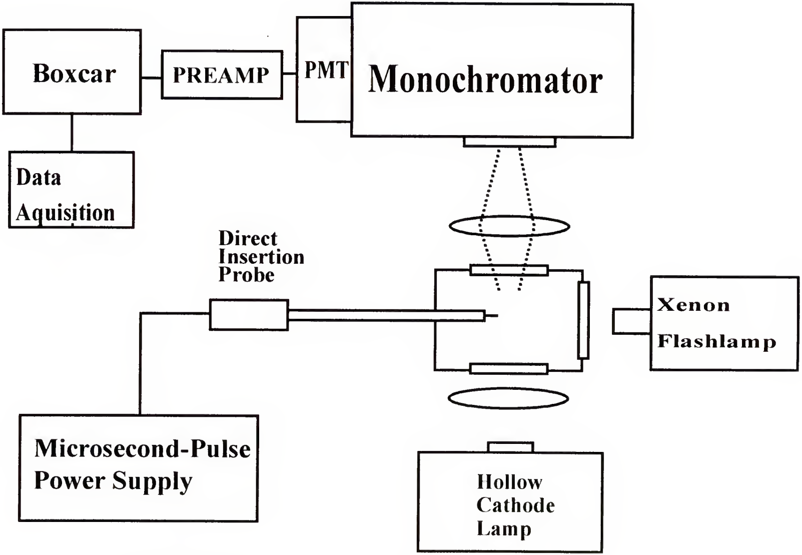

Fig. 31- Schematic diagram for optical spectroscopy with MPGD.

Xenon Corp., Woburn, MA, USA) was focused at ninety degrees to the monochromator and hollow cathode lamp. In each case, the analytical region was imaged onto the entrance slit of the monochromator.

A scanning monochromator was employed (EU-700,GCA/McPherson, Acton MA) having a grating with a blaze angle of 250 nm. A photomultiplier tube (Model R955, Hamamatsu, Bridgewater, NJ, USA) produced an output current converted to a voltage by a small transimpedance amplifier (Model A-1, Thorn EMI, Rockaway, NJ, USA). The signal was collected by a gated boxcar (Model 250, Stanford Research Systems, Sunnyvale, CA, USA). All spectra were digitized and sent to a computer via an analogue-to-digital converter (Model 245, Stanford Research Systems).

Whether the glow discharge was operated in the DC or pulsed modes, the sample was introduced into the source chamber by a direct insertion probe. A high voltage DC power supply (Model OPS-3500, Kepco, Flushing NY, USA) powered the discharge in the continuous mode. In the pulsed mode, a high power, pulse generator was employed (Model 350, Velonex, Santa Clara, CA, USA). The pulse width and frequency of the pulse generator were varied (1 - 300) μs and (5 - 5000) Hz, respectively, and voltages of up to 2500 V could be applied to the cathode. Due to the design of the Velonex power supply, no external regulator was necessary.

The glow discharge's pressure was optimized for emission with each sample and mode of power delivery. Comparisons were done at average power levels of 2.5 W and 25 mW for the DC and microsecond pulsed modes, respectively.

A machinable ceramic sleeve shielded the sample holder on the probe tip, allowing only 5 mm of the exposed 2 mm diameter cathode pin sample to be sputtered. The reference samples used in this work were brass (National Institute of Standards and Technology, NIST, Gaithersburg, MD, USA) Standard Reference Material SRM 1109 and Cu (99.999% pure, Johnson Matthey Chemicals). Ultra-high purity argon (99.995% pure, Alfagaz, Walnut Creek, CA, USA) was used as the sputter gas, as well as quartz windows and lenses to pass UV radiation.

The MPGD source was also used in combination with a quadrupole mass spectrometer. Time resolved studies of selected ions were performed by sitting on a particular m/z and profiling its evolution with respect to the initiation of the power supply. Gated spectra were taken using a detection system, centered around a waveform generator (Model HP3325A, Hewlett-Packard).[129] This generator produced a trigger that synchronized the applied voltage to the data collection time.

MPGD Emission

GDAES is a well-known method for the analysis of solid samples. The pulsed GD has been shown to exhibit many advantages in emission over DC-

GD. In this work, a high voltage, microsecond pulse power supply is used to drive the GD. The intense emission spectrum produced using this method is characterized and compared with the weaker DC-GD emission spectrum. Results have shown that MPGD atomic emission can be orders of magnitude more intense than that observed with DC-GDAES.

Operating in the DC and RF modes, the GD creates atoms and ions in a steady state manner. Upon pulsing a glow discharge the production of atomic species is halted, which shortens the duty cycle and the time available to extract a useful signal. Nonetheless, higher voltages are possible in the pulsed mode, which serve to induce larger comparable signals with a gated detection system.

A gated detection system permits temporal selection of the analytical signal. The data system collects the signal from the transducer only during a gated interval of the duty cycle, and discriminates against all signal and background incident at the detector outside the selected gate. Proper accumulation and averaging of the gated signal can result in a high signal-to-noise ratio for analytical measurements. More important, an adequately fast power supply is necessary to quickly ignite the discharge. It should have a short on-time and be able to sustain a high voltage across the discharge.

The Velonex pulse power supply used in these studies can drive the glow discharge to 4 amperes in a 200 ns risetime (Figure 32b). The current then drops to nearly zero and then rises in 2 µs to about one-hundredth of the original value, remaining at that current until the end of the pulse width. The subsequent loss in current after the initial breakdown may be an error in measurement, which was taken as a voltage drop across a 21 ohm-carbon resistor. Another possibility is that since electrons and ions have different mobilities, electrons account for the first peak and ions for the plateau. If a space charge is created, the second peak could be altered temporally by changing the discharge pressure, thus altering the length of the cathode dark space.

The trace in Figure 32a shows a voltage profile for the same 10-microsecond pulse used to obtain the current trace. Characteristic of pulsed discharges is the high leading edge of the voltage pulse, subsequently dropping toward a steady state level. The impedance of the discharge network extends the voltage decay for some period after pulse termination.

The rapid pulses occur on a time scale that allows investigation into critical events in the discharge, by observing emission profiles taken by imaging a spatial region very near to the cathode surface onto the entrance slit of the monochromator. Figure 33 displays an expanded view of the argon 419.8 nm emission verses current and voltage. The emission arises at 750 ns and before the current plateau; which indicates that the initial current spike is not an artifact; at least, there must be current flowing prior to the plateau period. The oscillations are due to rf noise because of the large initial current spike at the beginning of the pulse. Although emission from the argon fill gas is observed

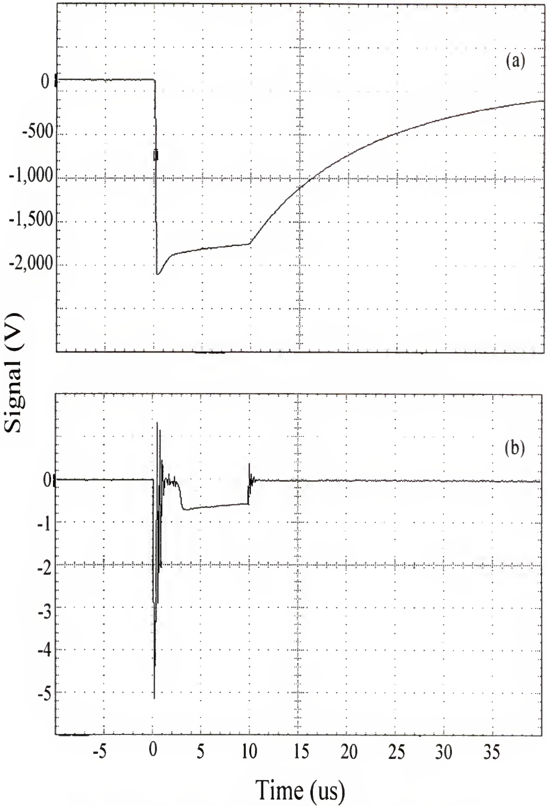

Fig.32- Current and voltage profile for a 10 microsecond pulse.

A) Voltage. B) Current.

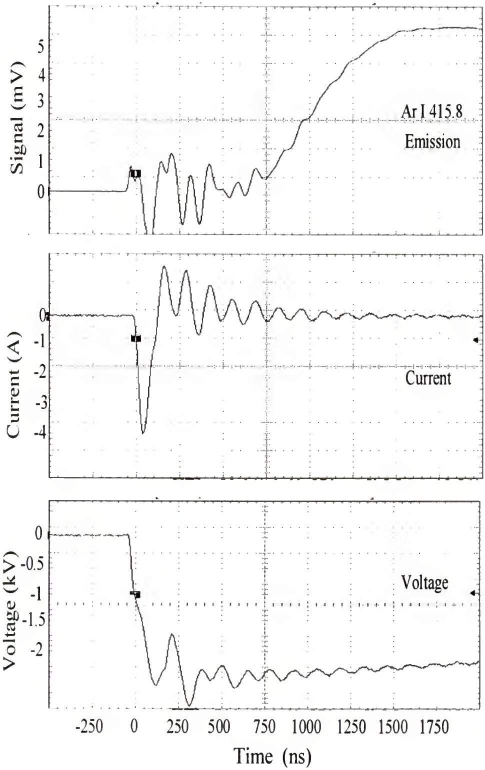

Fig. 33- Emission, current and voltage comparison soon after initiation.

soon after the discharge breaks down, emission from elements originating from the cathodic sample is delayed. First, the plasma must sputter away surface impurities, such as water vapor, then a sufficient quantity of sample atoms must also be sputtered and undergo collisions with electrons and metastable argon atoms to promote the emission seen in Figure 34 for copper at 327.4 nm.

Once the first copper emission is seen at approximately 2 microseconds, it maximizes at discharge termination after 7 microseconds. If argon ions indeed require nearly 2 microseconds to arrive at the cathode, as evidenced by the current pulse, then that event would be the rate determining step. The interruption of sputtering at the instance of termination results in an emission decay that is generally symmetrical to the growth in emission signal. By contrast, copper ion emission at 224.7 nm does not appear for another 2 microseconds later and, as shown in Figure 35, its signal remains strong much longer after the plasma is turned off.

The fast pulse discharge offers many opportunities to study plasma interactions. By setting a particular boxcar delay and scanning the monochromator, temporal spectral measurements can be taken. Figure 36 shows a series of temporal slices of emission taken for a copper cathode. The intensities of the lines change in relation to each other over the lifetime of the pulse. The most notable trend is that copper ion emission forms slightly later in the period and sustains its intensity after copper neutral atom emission has

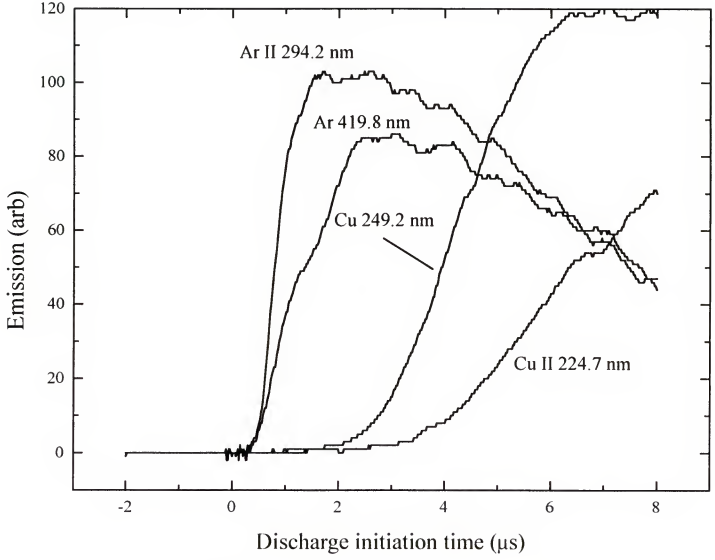

Fig. 34 Profile of various emission lines in MPGD.

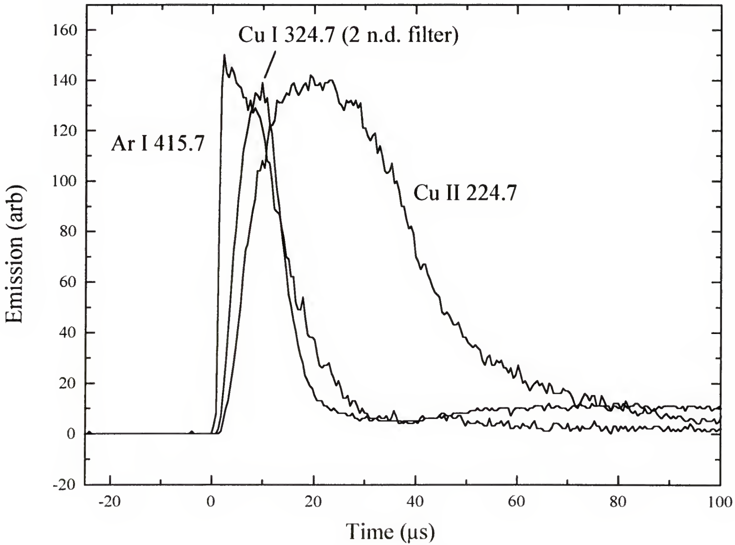

Fig. 35- MPGD temporal emission profiles.

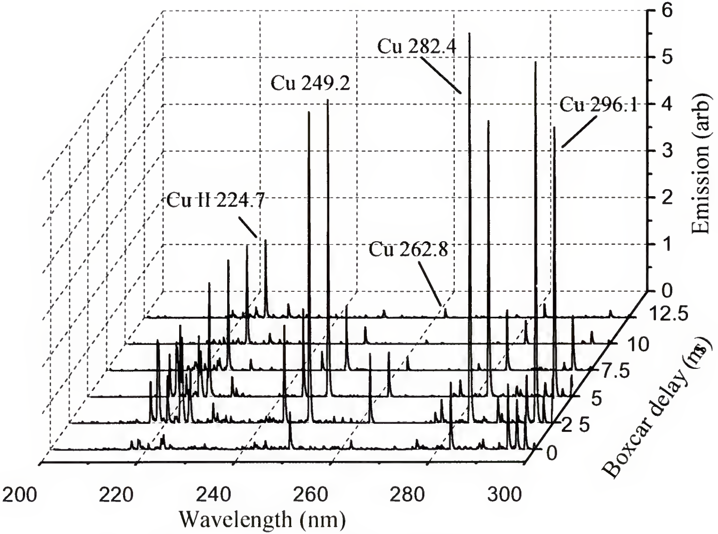

Fig. 36- Copper MPGD emission spectra for gated delay times.

dropped significantly.

A comparison of the spatial emission intensity of the sputtered species shows that MPGD is different than the DC-GD. In Figure 37, the copper signal is plotted for different distances from a 5 mm disk cathode with both the DC and MP modes. The MP emission drops off more rapidly upon moving toward the cathode, while the DC emission decreases much more slowly. Figure 38 is another emission profile, looking perpendicularly across a 2 mm diameter copper pin sample. Zero millimeters designates the center of the pin, while plus and minus 1 mm are at its edges. Copper emission drops off from the edges of the pin, as it had for the disk cathode, but the argon emission intensity is almost constant throughout the discharge. This is expected, since argon does not need to be sputtered and can be immediately excited by electron impact. The signal-to-background ratio is highest when looking at the edge of the cathode, despite its being the region of highest background. The decrease in emission when viewing the center of the pin is the result of a loss in total signal, some of which is lost that is blocked by the pin itself.

Pressure optimizations within the MPGD demonstrate a striking difference between it and DC-glow discharges. As seen in Figure 39, the emission signal is greatest at a pressure of about 3.5 torr and decreases steadily at higher pressures. This is in contrast to DC-GD, which has a maximum emission around 1.9 torr. The higher pressures and peak powers required suggest that MPGD

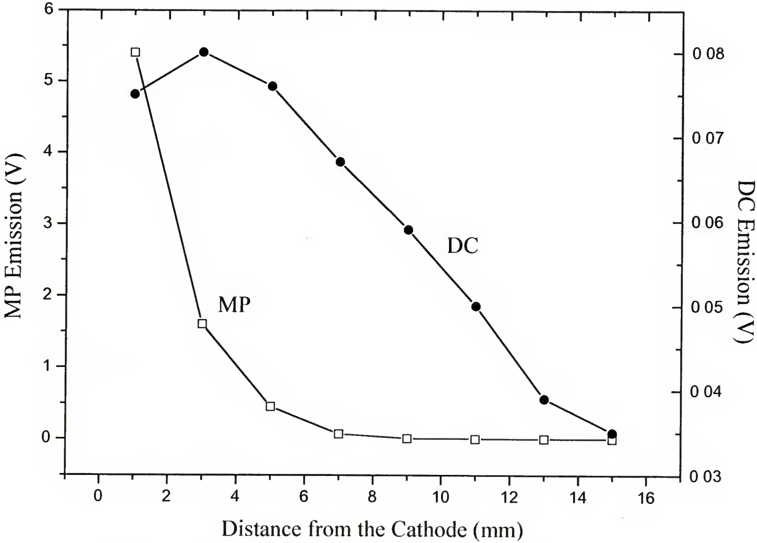

Fig. 37- Spatial Intensity profiles for the Copper 324.7 nm line; 1.6 torr, DC at 2.5 Watts, MP at 25 mW.

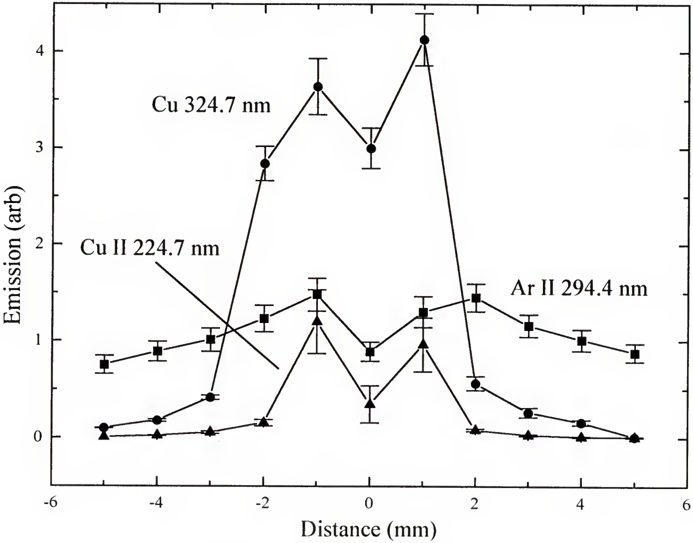

Fig. 38- MPGD emission profiles across an copper pin.

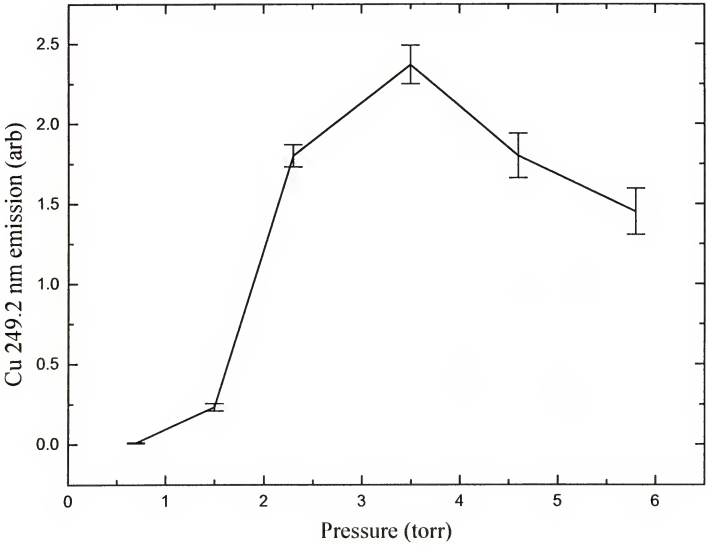

Fig. 39- MPGD Cu 249.2 nm emission vs pressure.

may act much more like an arc than does DC-GD.

Figure 40 is a plot of the emission signal vs. pulse frequency. The loss in the signal with higher pulse rates is related to the time needed to recharge the power supply's capacitor. Higher frequency offers an advantage of greater signal averaging; increased RSDs and lower emission intensities may degrade signal-to-noise ratios and preclude the use of high frequencies.

The relationship between pulse width and emission signal is given in Figure 41. The boxcar gate is limited to 10 μs. Signal R.S.D. varied little for changes in pulse width, although the signal varies by almost an order of magnitude when the pulse width changed from 1 - 10 μs. Analyte emission intensities are a function of the power supply and the amount of current it can deliver during each pulse.

Frequency and pulse width are the major factors in determining the average power delivered to the discharge. With a copper cathode, the average power is approximately 2.5 W with a 10 μs pulse width and at 2.0 torr. While this is a common power setting with a DC-GD, the average power with MPGD is not related to the emission signal acquired as it is with DC-glow discharges. For example, setting the frequency to 25 Hz would give only 25 mW average power. At this power, the gated emission intensity actually increased (Fig. 40), even though the plasma was not perceivable by the eye at this frequency. At 2.5 W, the MPGD plasma appears as bright as a 2.5 W DC plasma. Since a DC-GD

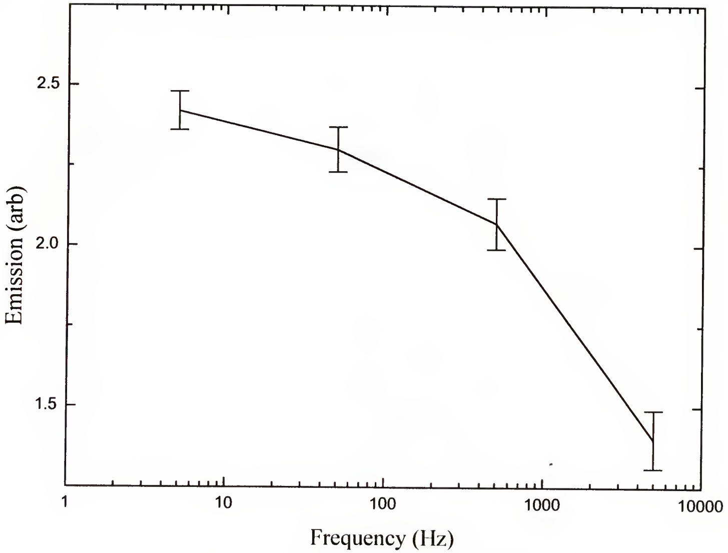

Fig. 40- Copper MPGD 249.2 nm emission verses frequency.

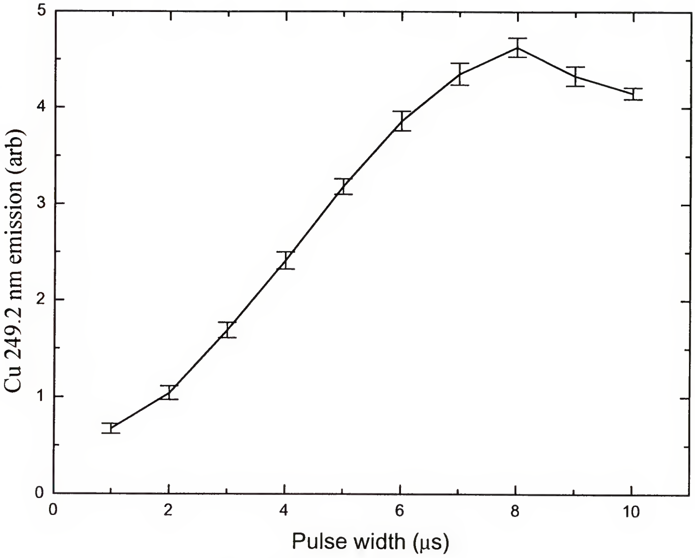

Fig. 41- MPGD Cu 249.2 nm emission verses pulse width.

cannot be initiated at 25 mW, comparisons between these two modes at equivalent powers are difficult to make.

Analytical Merits

The analytical potential of the fast pulse discharge is reflected in the high emission intensity measured during the on-cycle. Even though the average power of the pulsed discharge is a hundred times less than DC, the peak emission is orders of magnitude greater than observed in the DC mode. From atomic absorption measurements, this enhancement is a result of a rise in sputtering during the high current pulse and the instantaneous high current which pulse more readily promotes atomic excitation for each atom produced.

By use of a gated detector, an advantage to pulsing the discharge can be gained, as shown in Figure 42, a comparison of results from an NIST 1109 brass sample. Note the difference in scales between the two spectra, as well as the different ratios of lines; in addition the major copper peaks at 324.7 nm and 327.4 nm are saturated in the pulsed discharge spectrum.

The MPGD excites atomic emission more effectively than does DC-GD. In Figure 42, copper emission spectra are compared for the two modes. The pulsed spectrum exhibits differences from the DC spectrum. The most important is that the atomic line intensities increase by 50 - 400 times from those observed with a DC- GD; the ion line intensities increases by only 10 times. It should be noted that the relative ion-atom ratio is dependant on the working pressure; the pressure was optimized for the atom lines.

The calibration curve given in Figure 43 was obtained for zinc in brass using DC-GDAES and MP-GDAES. The calibration curves are linear at high concentrations and becoming nonlinear at low concentrations where the background emission dominates the signal. Background emission lines from water and argon do not increase as quickly as does emission for analyte species for MPGD. The signal is about two orders of magnitude more intense with MPGD, however, DC-GD exhibits a background emission which is an order of magnitude less than with MPGD. The zinc emission L.O.D. is nearly ten times higher for the MPGD as compared to the DC-GD.

Plasma Diagnostics

There may be some question whether the MPGD plasma deserves the title of 'glow discharge.' Boumans describes discharge parameters as a function of the current induced.[13] He ascribes an arc to any plasma with a current above one ampere. It is possible that this assignment may only apply to discharges run in a DC mode. Even though the initial current is greater than 1 ampere, it does reach a steady state value of less than 50 mA after 2 microseconds in which the discharge could be called a glow discharge even under Bouman's definition. Furthermore, when the MPGD is operated at powers similar (2.5 W) to a DC discharge, the two plasmas are virtually indistinguishable in intensity and color.

Besides the analytical capability of the microsecond pulsed discharge, it

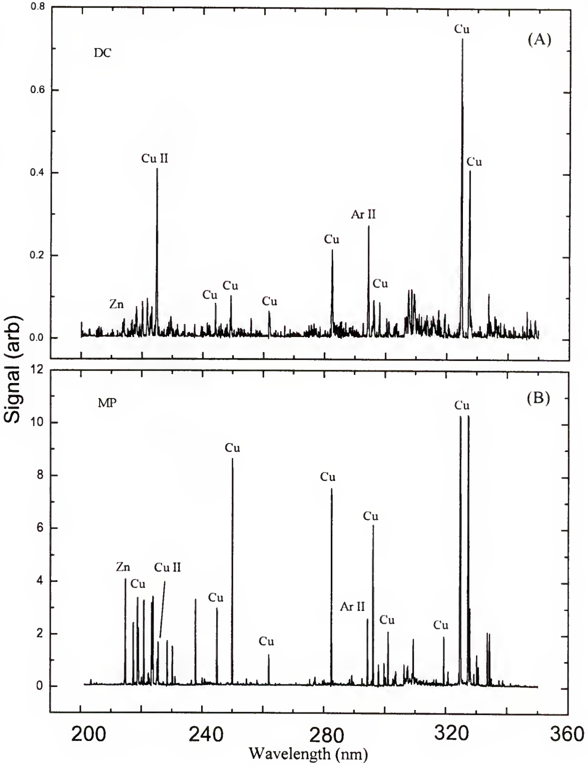

Fig. 42- Brass NIST #1109 emission spectra, (a) DC emission at 25 W, (b) MP emission at 25 mW.

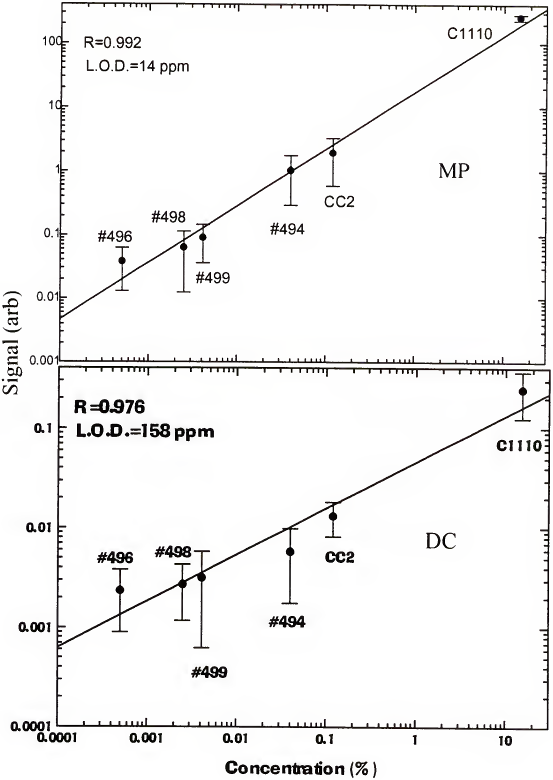

Fig. 43- Calibration curves for zinc in copper.

can be used to obtain interesting and valuable diagnostic information about glow discharges processes. Given that the MPGD is a true glow discharge, its fast turn-on times can be used to uncover temporal events related to all GD plasmas. The main objective of this section is to characterize these processes and to understand the dynamics of important plasma species.

Mass Spectrometry

With optical spectroscopy, the high velocity of photons allows for the use of a boxcar integrator for recording fast, transient events occurring in the pulsed glow discharge. However, the acquisition of temporal mass spectra is complicated by the slow transit time of ions compared to photons. Ion movement is diffusion limited at 1 torr; in the GD, the cathode is normally positioned about 1 cm from the ion exit orifice. Before a signal can be observed the analyte atoms must first be sputtered and then diffuse across the GD cell to the orifice, be ionized there and be extracted as ions into the mass spectrometer. Figure 44 distinguishes the ion profiles of gaseous argon and of copper atoms that originated from the sample for different ion exit orifice distances. The changing distance does not affect the population of argon ions near the exit orifice, and results in overlapping ion profiles. These ions need only to enter the mass spectrometer and travel to the detector to be measured. They are first seen about 75 microseconds after discharge initiation. Over the next several hundred microseconds, the ion signal reaches a maximum and then exhibits a long tail

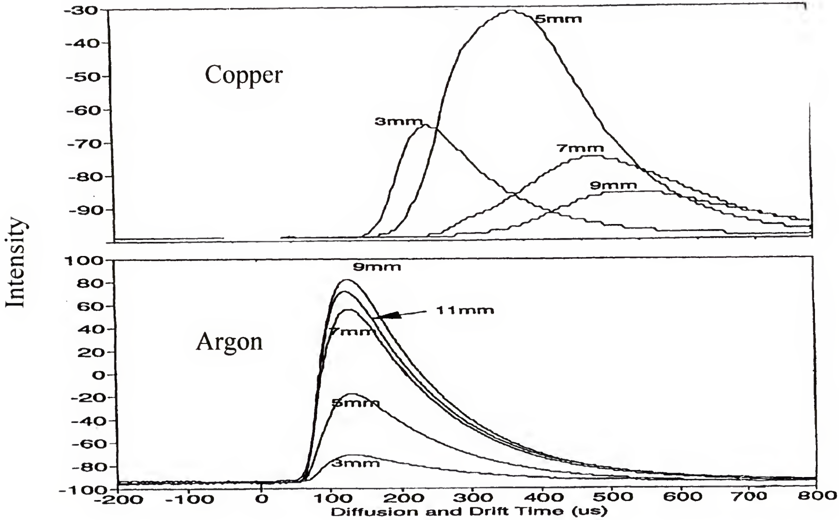

Fig. 44-.Mass Spectrometry profiles vs. extraction distance for a copper sample.

before again attaining background levels.

Copper atoms may be extracted by the exit orifice only after they have been sputtered and diffuse across the discharge cell. Increasing the cathode to ion orifice distance induces a shift in the transit time required to reach the detector. The extended ion signal produced with a ten millisecond initial pulse is most likely the result of a random walk the atoms experience through collisions in the gaseous medium; therefore by injecting ions into the system by means of a short energetic pulse, diffusion phenomena in the glow discharge can be studied.

The fast pulse discharge produces an intense ion spectrum, despite the fact that the initial ion packet is spread because of the diffusion processes. The signal from a 10 microsecond pulse may extend to nearly one millisecond, depending on distance. Mass spectra have been sampled temporally by delaying the gate over a given interval after discharge initiation. Figure 45 gives several spectral profiles that reveal time dependent processes with an iron NIST #661 sample. Initially, only background impurity gas can be found in the spectrum, followed by a decrease in these species and an increase in the iron signal. Using a proper delay time, the GDMS spectra can be optimized to discriminate against background gases which are first to reach the detector.

Secondary electrons released from collisions of primary electrons with argon have a mean energy of around 2 eV and are not energetic enough to

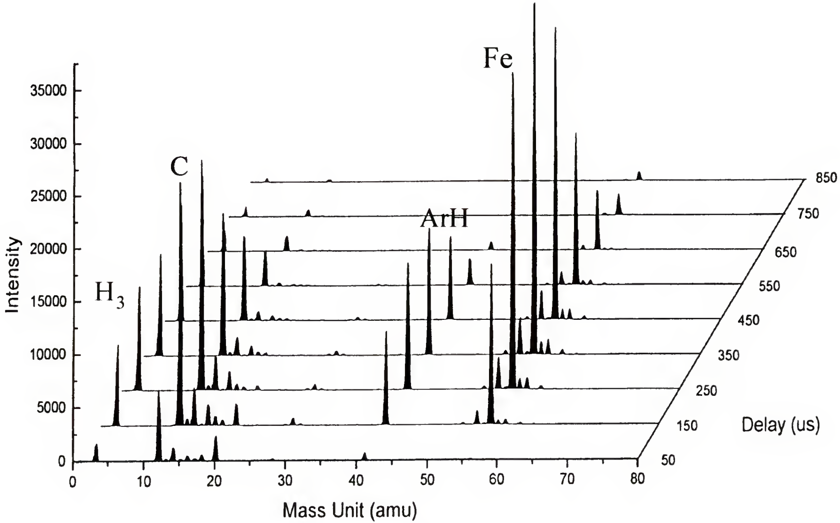

Fig. 45- MPGD/MS spectra for Iron NIST #661, 1.0 torr, 600 Hz, 7mm from orifice.

ionize most elements.[3] Nonetheless, they may interact with lower energy states of sputtered species thus promoting atomic emission and ionization. The mean energy distribution of secondary electrons may be increased through coulombic interactions between them and high energy, primary electrons passing through the negative glow.[137] During the initial breakdown of the microsecond pulse, the current increases to 4 amperes, producing a large number of secondary electrons are formed. The current then drops to 50 mA due to electron collisions, resulting in a lowering of the mean electron temperature. During the plateau region, there is not only a large number of electrons available for recombination, but also a considerable argon metastable population.

The sputtered atoms arrive in the plasma within a few milliseconds and undergo electron impact and ions undergo electron recombination, resulting in atomic emission. Farnsworth and Walters postulate that electron impact is too low in energy to cause much ionization in a microsecond pulsed hollow cathode.[138] Accordingly, the major pathway to ionization of sputtered atoms is through an interaction with argon metastables. This would explain the longer appearance time for copper ion emission, since collisional transfer of energy from a metastable has a lower cross-section than electron impact.

Temperature Measurements

Rotational temperatures are considered good measures of the thermal temperature of a plasma.[139] Their determination entails recording a number of emission lines within a single band of a molecular species. The ratio in intensities of the sidebands can be plotted to yield a slope related to the thermal temperature according to a Boltzmann distribution.

N_2^+ is a commonly used molecular specie for rotational temperature calculations. It is normally present in the glow discharge plasma as a trace impurity, but its bands are too weak to be resolved for use in temperature measurements. Nitrogen was added to the argon discharge to a partial pressure of 10% to produce intense enough emission signals for the work reported here.

A 0.5 m (Model 82-516, Jarrell Ash, Monrovia, CA, USA) monochromator had sufficient resolution to resolve the R branch transitions of the N_2^+ band emission for temperature calculations. Figure 46 is the N_2^+ emission spectrum obtained upon viewing the cathode approximately 1 mm below a copper disk cathode. The transition lines that were used for the calculation are labeled.

A Boltzmann plot for the determination of the N_2^+ rotational temperature is shown in Figure 47. The first three points in the upper left were calculated after first correcting for the background. The slope has a linearity of R=0.9992 and the temperature is found to be 478 K. The MPGD rotational temperature is nearly 200 K lower than that found with a DC-GD under similar conditions. With 10% nitrogen in argon, a rotational temperature of 660 K was calculated at 0.5 mm from the cathode surface for DC-GD.[140] This is surprising, since the emission intensities are so much higher for MPGD. However, the GD is not in

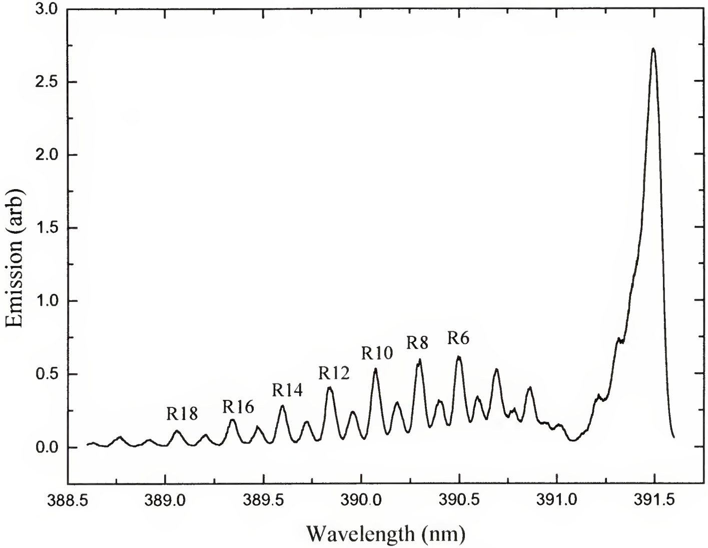

Fig. 46- MPGD N_2^+ emission spectrum with a copper cathode, 10% nitrogen, 0.9 torr.

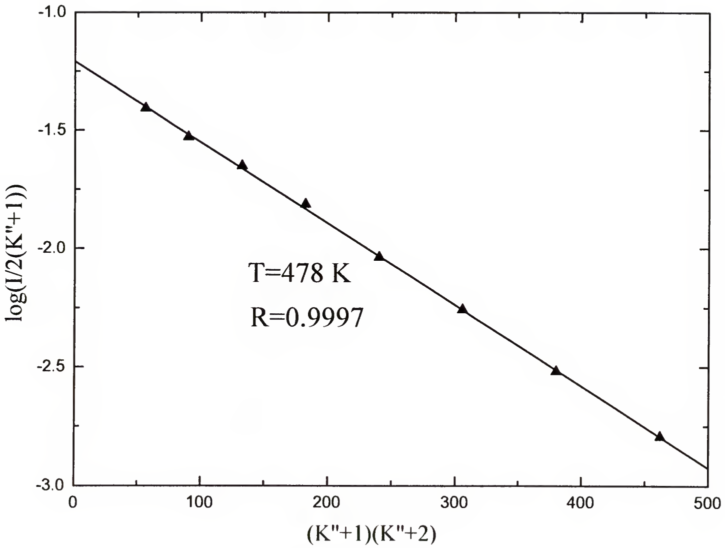

Fig. 47- Boltzmann plot for the MPGD rotational temperature.

thermal equilibrium and other temperatures, such as electronic, may be much greater.

Atomic absorption

Emission occurs primarily during the microsecond pulse. Figure 48 shows a quite different response of ground state atoms compared to their excited analogues, but the atomic population seems to last many milliseconds after the discharge terminates. When imaging the cathode directly, copper 324.7 nm emission has a F.W.H.M. of about 20 microseconds for a 10 microsecond pulse (Figure 35), while the ground state copper population has a halfwidth of 2 - 3 ms and decay times from 10 - 12 ms. This reflects a diffusion controlled process of the sputtered atoms which are ejected from the cathode; the sputtered atoms drift into the negative glow, and into the analytical volume sampled in Figure 48.

A 300 microsecond pulse width is optimum for peak atomic absorbances; longer pulse widths result in higher sputter yields. Figure 49 depicts an atomic absorbance plot using a hollow cathode lamp in the MPGD at 30 Hz. At this repetition frequency, the average MPGD atomic population determined is not as high as with DC-GD at any pulse width for the MPGD. However, pulse repetition rates greater than 100 Hz cause residual sputtered atoms to merge and be detected after following pulses. From atomic absorption studies, the absorbance exceeds that of DC-GD at equivalent power levels.[141] Also, from Figure 50,

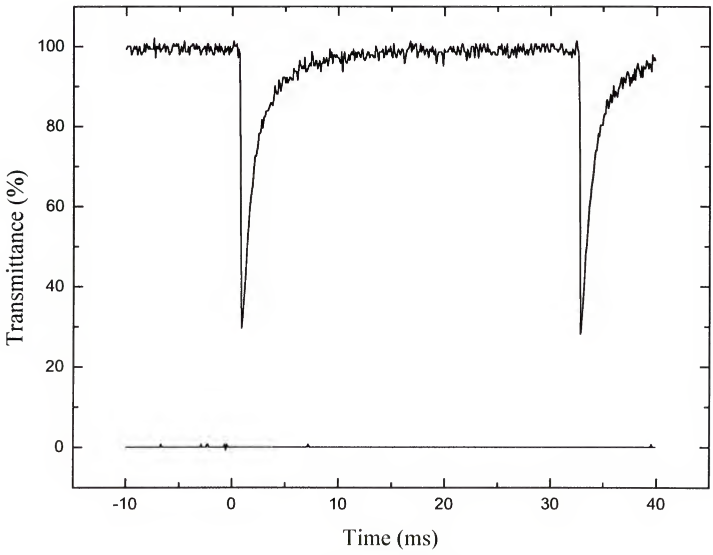

Fig. 48- MPGD Copper absorption profiles for 10 μs pulses

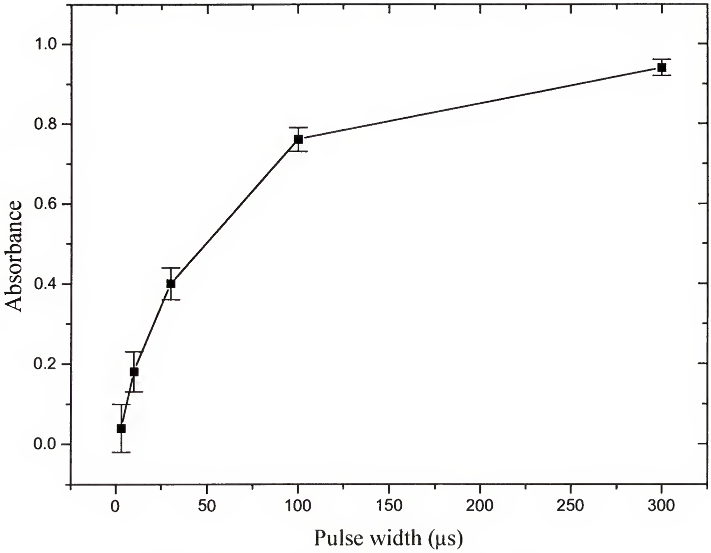

Fig. 49- Peak absorbance plot at various power supply pulse widths.

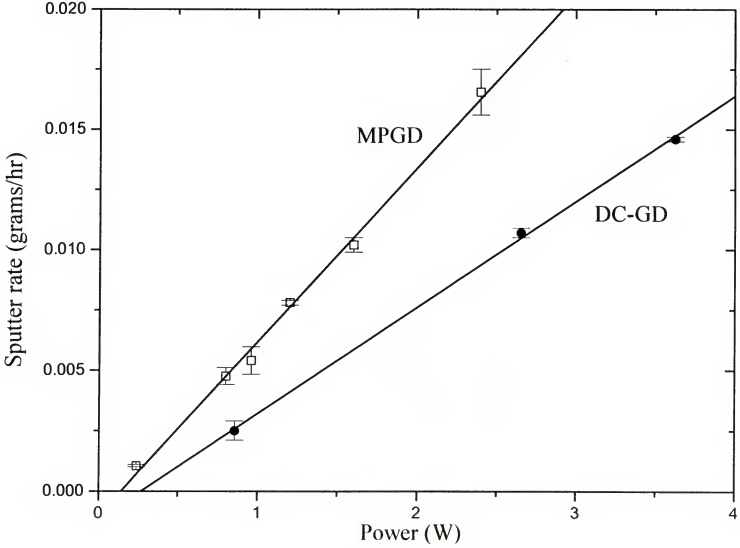

Fig. 50 Sputter rate comparison for DC and MP modes.

MPGD is shown to produce 2 - 3 times more atoms from a copper cathode as compared to DC over the entire range of powers studied.[141]

The profile in Figure 48 was taken by directly observing the cathode surface. Emission saturates the detector after the discharge turns on, but this cannot be seen on the time scale shown. The absorbance is observed to peak about 1 ms after the pulse initiates. This delay in the onset of absorbance is artificial, because when looking very near to the cathode, emission is strong and interferes with the absorption. Figure 51a is a simultaneous trace of absorption and emission with a copper cathode. Figure 51b was obtained by subtracting out the emission response, revealing the expected drop in atomic population that occurs during the on-time of the pulse. The atomic fluorescence spectra in Figure 52 support the results found by atomic absorbance. These spectra were taken 5 mm away from the cathode and the highest intensities are observed 4 milliseconds after discharge initiates. The delay accounts for the time required for the atoms to diffuse into the analytical region.

Diffusion Studies

The peak absorbance, fluorescence, and decay times are directly related to normal rates of atomic diffusion. A 5 mm copper disk was used to experimentally determine peak absorbance times. Figure 53 shows copper 324.7 nm absorbance profiles as the direct insertion probe is moved from 7 - 15 mm from the cathode. As the probe is moved farther away from the analytical

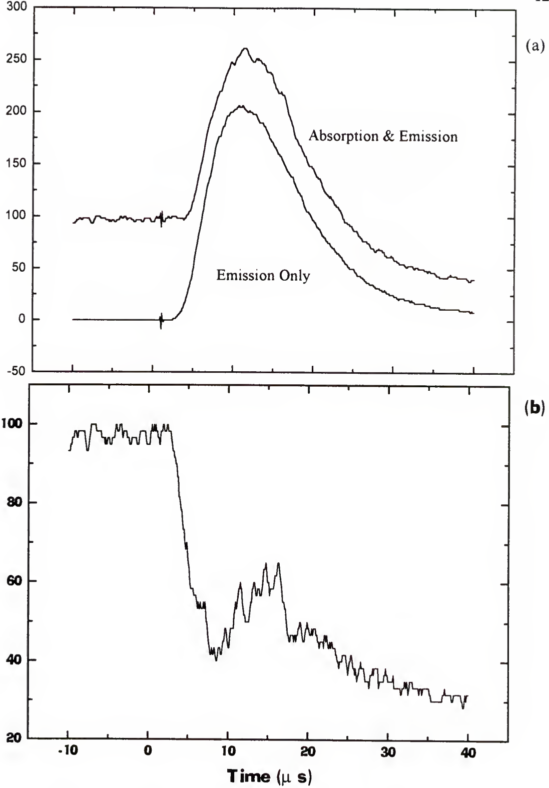

Fig. 51- (a) MPGD absorption and emission profiles Cu 324.7 nm
(b) MPGD absorption profile emission was subtracted out.

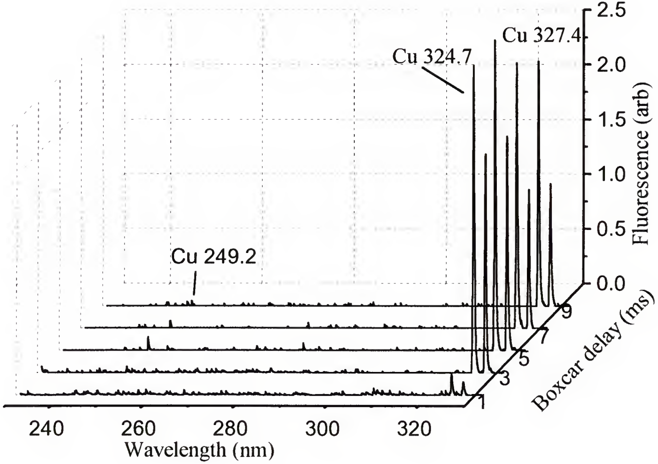

Fig. 52- Copper fluorescence profiles at various boxcar gate delays.

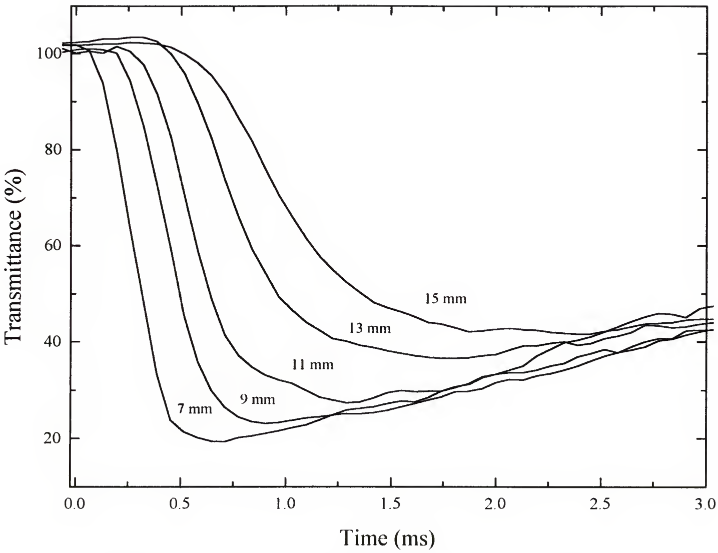

Fig. 53- Copper absorption profiles vs distance from cathode. 1.6 torr. 100μs pulse.

region, the atoms require longer diffusion times. Distances shorter than 7 mm are anomalously shifted to longer times due to an interference from emission.

Theoretical peak absorbance times can be derived from a simple diffusion model. The equation for the diffusion coefficient for a binary system (copper and argon) is given as:

$$D=\frac{3(2\pi k^3 T^3/\mu)^{1/2}}{16P\pi\sigma^2} \tag{4-1}$$

where k is the Boltzmann constant (J/K), T is the thermal temperature (K), μ is the reduced mass of the collision partners (Kg), P is the pressure (Kg/cm^2) and σ is the collision cross section (cm^2). The value for σ was calculated using equation 1-2 and given a mean free path of 0.005 cm. The discharge was operated at 1.5 torr and the temperature was assumed to be 500 K from thermal values determined from N_2^+ rotational spectra.

If the geometry of the atom source is assumed to be an infinite plane and for given a point detection,[142] the diffusion equation would be related to the distance from the source (r) and the time after the atomic production by:

$$c(r,t)=\frac{c_o}{2(\pi D t)^{1/2}}e^{-\frac{r^2}{4Dt}}. \tag{4-2}$$

To find an equation for the time of maximum absorbance, the partial derivative with respect to time is taken resulting in

$$\frac{\delta c(r,t)}{\delta t}=\frac{-c_o}{4(\pi D)^{1/2}t^{3/2}}e^{\frac{-r^2}{4Dt}}+\frac{r^2C_o}{8\pi^{1/2}D^{3/2}t^{5/2}}e^{\frac{-r^2}{4Dt}} \tag{4-3}$$

the minimum is found by setting the rate to zero and solving the equation for t, obtaining the following equation:

$$t^{\max}=\frac{r^2}{2D}. \tag{4-4}$$

Figure 54 compares the uncorrected experimental and calculated peak absorbance times at different distances from the cathode. The values are in good agreement for distances greater than 5 mm. Since the original equation was patterned after a source with dimensions of an infinite plane, a calculation error would result for distances far away from the cathode because it becomes more like a point source instead of a infinite plane.

In the pulsed mode, the cathode appears smoother after sputtering than with equal exposure times in the DC-GD. This can be attributed to a lower sputter rate and/or partial melting the surface. There is also a concern that thermal emission is a prominent mechanism for atomization using MPGD. However, the cathode is not warm to the touch immediately after sputtering, this is valid for cathodes operated at 2.5 W in the DC mode. The question of whether the cathode is hot enough for thermal vaporization on the microsecond time scale with MPGD, can be resolved by further research on the sputtering of refractory metals.

Nonconductors

Thus far, the only way to analyze a pure nonconductor by a glow discharge has been to apply an RF field. Using MPGD, a plasma has been obtained with the ceramic Macor (Figure 55). A weak plasma could be observed when the voltage was set at 2500 V. Although Macor has aluminum and magnesium at concentrations of 10.1% and 9.9%, respectively, only argon and water emission lines could be seen in an emission spectra.

If there is any aluminum emission at 309.1 nm and 308.2, it is obscured by a large OH band. Similarly, magnesium emission should appear at 285.2 nm but this also falls in the region of another OH band. The remainder of the spectrum is dominated by argon ion emission; the two strongest of which are shown at 294.4 and 297.1 nm. Until emission from elements originating from the sample is seen, we cannot be certain that sputtering occurs.

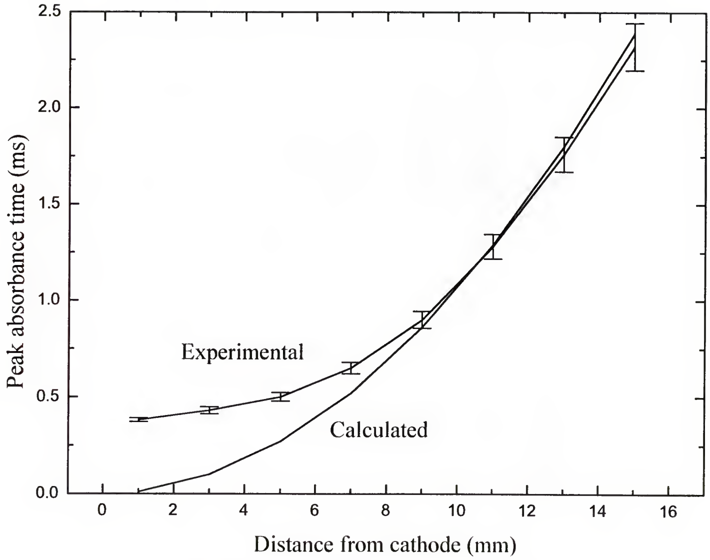

Fig. 54- Peak experimental and calculated MPGD absorption times

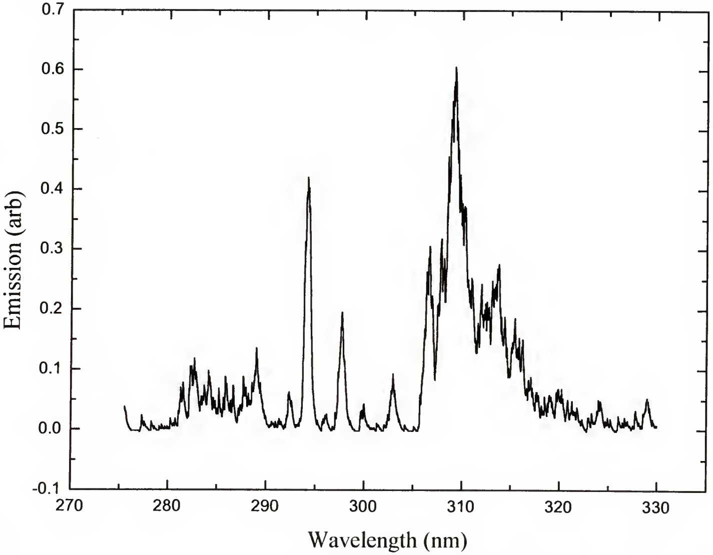

Fig. 55- MPGD spectrum for MACOR taken at 1.5 torr and 2.5 watts.

CHAPTER 5
CONCLUSIONS

The GD has been shown to be a useful atom source for the direct sputtering of solid samples for atomic fluorescence spectrometry. Conventional, broadband light sources have advantageous features for an inexpensive, GDAFS technique with capability for multielement analysis. In this work, the xenon arc lamp and xenon flashlamp were used as spectral continuum sources.

Multielement GDAFS has proven to be an interesting alternative to GDAES. The low energy GD plasma leaves a majority of its atoms in the ground state or a low lying electronic state, resulting in a much simpler metal fluorescence spectrum than observed in emission. Observed fluorescence spectra appear relatively free of both the argon fill gas emission lines and molecular impurity bands that often obscure trace metal detection in GDAES.

The pulsed glow discharge has been found useful as a source for fluorescence methods. After the plasma is extinguished, the emission decays rapidly while the atomic population diffuses at a slower rate. This creates a dark period where atomic fluorescence can be probed without being affected by emission. The more intense flashlamp is preferred in comparison to the arc lamp. Simultaneously pulsing the glow discharge and delaying the flashlamp gives a larger signal-to-background ratio resulting from a reduction in emission background.

In addition, fluorescence measurements assist in the fundamental studies of the glow discharge plasma by monitoring metastables and molecular species, such as metal oxides and metal atom populations. Ionic fluorescence has not been observed using the arc lamp for two main reasons: first the glow discharge produces a small ionized population, about 1%, and second the arc lamp is not of sufficient spectral radiance. The detection of ion lines in these spectra with flashlamp excitation can be attributed to the ionic number density, to the strength of the lines, and to the high intensity output of the flashlamp.

Improvement in detection limits may be possible by reduction of the limiting noises such as scatter and background emission. Other interferences may become apparent if the limiting scatter background can be significantly lowered. In any case, the number of spectral interferences will be generally less than that suffered with GDAES. More modifications of the glow discharge are required to reduce the scatter background to dark current levels. Scattering can be lowered further by reducing the reflectivity of the anode chamber and window. Also, a more effective beam dump than the Wood's horn could be fitted.

Multielement GDAFS is not yet competitive with GDAES and GDMS for absolute detection limits. Comparisons between these two were made at a disadvantage to GDAES, since it is best observed with a hollow cathode type discharge. Presently, multielement GDAFS can offers quick identification of major and minor metallic species in many different conducting matrices.

Studies on the advantages of simultaneously measuring mass and fluorescence spectra are possible. A mass spectrum tends to contain some molecular interferences for atomic peaks, which may be resolved by comparison to a fluorescence spectrum. The broadband output of the flashlamp may also nonselectively increase ion concentrations in the plasma, making the mass spectrometer more sensitive, by promoting atoms to the ionization limit.

The use of a high power, short pulse to drive a glow discharge has several interesting features that merit further exploration. MPGD spectra taken with a quadrupole mass spectrometer are equivalent in intensities to that of DC-GDMS, though this type of mass spectrometer works best with continuous sources. Full advantage of the short term nature of the MPGD ion signal can be made by coupling with a time-of-flight or ICR mass spectrometer.

Enhanced atomic excitation could make glow discharge atomic emission more competitive with glow discharge mass spectrometry for elemental sensitivity. Beyond analytical advantages, a fast pulse discharge permits diagnostic evaluations of plasma processes that aid our understanding of the glow discharge.

The advantage of atomic emission measurements compared to mass spectrometry is the immediacy of observation, with no lengthy mass transport of ions during which time resolution is lost. Atomic diffusion processes have been followed by absorption methods to gain some measure of sputtered atom densities as a function of time.

The MPGD has provided an opportunity to study how atomic and excited state populations are introduced into the plasma. Using atomic emission, spatial and temporal distributions of energetic species were mapped. The emission extends over the GD on-time, but absorbance and fluorescence studies revealed an atomic population that decays on a millisecond time scale. However, the measured atomic concentration was found to be in good agreement with theoretical models for diffusion with rigid spheres.

A more precise temporal and spatial map of the MPGD plasma may offer insights into the dominant processes for sputtering and excitation. Penning ionization, electron impact and metastable formation can be examined more closely than had been possible with DC glow discharges. Due to the extensive delay in ion emission, Penning ionization appears to be a dominant pathway for ion formation. Mainly, argon metastables are not destroyed by electron impact after termination of the GD power , allowing the Ar metastables to interact with gaseous species though collisions and charge transfer.

The results imply that MPGD produces simpler spectra with greater intensity than the DC-GD. Lower average powers permit longer analysis times and consume less sample. The rapid sputtering with MPGD may allow studies for the understanding of basic processes occurring during the establishment of the plasma. Also, the collapsing discharge may reveal evidence about the pathways in which thermal equilibrium is reestablished. From rotational temperatures measurements, the MPGD appears to be thermally cooler than the DC-GD by nearly 200 K. If electron temperatures are similar, then the atomic population must be temporally much higher in the MPGD mode to obtain a more intense emission spectrum.

In the search for the perfect atom source, the accommodation for any type of sample is a requirement. DC-GD falls short of this goal since it can only analyze conducting samples. It is encouraging that MPGD can establish a plasma at all with Macor. However, the emission intensity is very weak. Perhaps the surface of the nonconductor retains a positive charge that repels argon ions. If this is true, the surface could be pre-neutralized by an electron beam before each pulse. Another possibility is reducing the thickness of the sample, so that a higher potential could be applied to the sample's surface.

REFERENCES

1. Harrison, W .W.; Prakash, N. J. *Anal. Chim. Acta* **1970**, 49, 151.
2. Westwood, W. D.; *Progress in Surface Science* **1972**, 7, 71.
3. Chapman, B. *Glow Discharge Processes*; Wiley: New York, 1980.
4. Omenetto, N.; Smith, B. W.; Winefordner, J. D. *Spectrochim. Acta* **1988**, 43,1111.
5. Marcus, R. K.; Harrison, W. W., *Anal. Chem.* **1987**, 59, 236.
6. Stirling, A. J.; Westwood, W. D. *J. Phys. D.* **1971**, 4, 246.
7. Chakrabarti, C. L.; Headrick, K. L.; Hutton, J. C.; Bicheng, Z.; Bertels, P. C.; Back, M. H. *Anal. Chem.* **1990**, 62, 574.
8. Gough, D. S.; Hannaford, P. and Lowe, R. M. *Anal. Chem.* **1989**, 61, 1652.
9. Bengtson, A.; *Spectrochim. Acta* **1991**, 40B, 631.
10. Harrison, W. W.; Loving, J. *Anal. Chem.*, **1983**, 54, 1523.
11. Hess, K. R.; Marcus, K. R. *Spectrosc.* **1987**, 2, 24.
12. van Dijk, C.; Smith, B. W.; Winefordner, J. D. *Spectrochim. Acta* **1982**, 37B, 759.
13. Boumans, P. W. J. M. *Anal. Chem.* **1972**, 44, 1219.
14. Mitchell, D. G.; Johansson, A. *Spectrochim. Acta* **1990**, 25B, 175.
15. Kagan, Y. M.; Cohen, C.; Avivi, P. *J. Appl. Phys.* **1988**, 63, 60.
16. Perreira, N. P.; Strauss J.A.; Human, H. G. C. *Spectrochim Acta* **1983**, 38B, 899.

17. Fang, D. C.; Marcus, R. K., J. Anal. Atom. Spectrosc. **1988**, 3, 873.

18. Caroli, S.; Senofonte,O.; Violate, N.;Astrologo, R. *J. Anal. Atom. Spectrom.* **1988**, 3, 887.

19. Russell, B.J.; Walsh, A. *Spectrochim. Acta*, **1959**, 15, 883.

20. Coburn, J. W.; Kay, E. *Appl. Phy. Lett.* **1971**, 19, 350.

21. Harrison, W. W.; Magee, C. W. *Anal. Chem.* **1974**, 46, 461.

22. Coburn, J. W.; Kay, E. *Appl. Phy. Lett.* **1971**, 18, 435.

23. Watson, C. H.; Wronka, J.; Laukien, F. H.; Barshick, C. M.; Eyler, J. R. *Spectrochim. Acta* **1993**, 48B, 1445.

24. Watson, C. H.; Wronka, J.; Laukien, F. H.; Barshick, C. M.; Eyler, J. R. *Anal. Chem.* **1993**, 65, 2801.

25. Sanderson, N.E.; Hall, N.E.; Clark, J., Charalambous, P.; Hall, D., *Mikrochim Acta* **1987**, 1, 275.

26. Jakubowski, R.; Stuewer, D.; Vieth, W., *Anal. Chem.* **1987**, 59, 1825.

27. Robinson, K.; Hall, F.H., *J. Metals* **1987**, 39, 14.

28. McLuckey, S. A.; Glish, G. L.; Asano, K. G.; Grant, B. C. *Anal. Chem.* **1988**, 60, 2220.

29. McLuckey, S. A.; Glish, G. L.; Asano, K. G. *Anal. Chim. Acta* **1989**, 225, 25.

30. Chambers, D. M.; McLuckey, S. A.; Glish, G. L. *Anal. Chem.* **1993**, 65, 778.

31. Lauritsen, F. R.; Choudhury, T. K.; Dejarme, L. E.; Cooks, R. G. *Anal. Chim. Acta* **1992**, *266*, 1.

32. Winefordner, J. D.; Vickers, T. J. *Anal. Chem.* **1964**, 36, 1939.

33. Shick, C. R.; Raith, A.; Marcus, R. K. *J. Anal. Atom. Spectrosc.* **1993**, *8*, 1043.

34. Ingle, J. D. Jr.; Crouch, S. R. *Spectrochemical Analysis*; Prentice-Hall: Englewood Cliffs, NJ, 1988.

35. Williams, R. *Appl. Spectrosc.* **1989**, 43, 1409.

36. Howatson, A. M. An *Introduction to Gaseous Discharges*, 2nd ed.; Pergamon: New York, 1976.

37. Valyi, L. *Atom and Ion Sources;* Wiley: New York, 1977.

38. Brown, S. C. *Introduction to Electrical Discharges in Gases*; John Wiley and Sons: New York, 1966.

39. Aston, F. W. *Roy. Soc. Proc*, **1910**, 84, 526.

40. Little, P. F.;von Engle, A. *Proc. Royal Soc.* **1954**, 224A, 209.

41. Fang, D.; Marcus, R. K. "Fundamental Plasma Processes,"*Glow Discharge Spectroscopies*; Marcus, R. K., Ed.; Plenum Press: New York, 1993.

42. Llewellyn-Jones, F. *The Glow Discharge.* Wiley; New York, 1966.

43. Langmuir, I. *Phys. Rev.* **1925**, 26, 585.

44. Anderson, J. M. *J. Appl. Phys.* **1960**, 31, 511.

45. Fang, D.; Marcus, R. K. *Spectrochim. Acta.*, **1990**, 45B, 1053.

46. Wehner, G. K.; Anderson, G. S. *Handbook of Thin Film Technology*; L. I. Maissel and R. Glang, Ed.;McGraw-Hill Co.: New York, 1970.

47. Harrison, W.W.; Bentz, B. L. *Prog. Anal. Spectrosc.* **1988**, *11*, 53.

48. Wehner, G. K. *Methods and Phenomenoma*, Vol. 1; Wolsky, S. P.and Czanderna, A. W., Eds.; Elsevier Scientific: New York, 1975.

49. Carter, G.; Nobles, M. J.; Katardjiev, I. V. *Vacuum* **1988**, 38, 479.

50. Coburn, J. W.; Harrison, W. W. *Appl. Spectrom. Rev.* **1981**, 17, 95.

51. Bernhard, A. E. *Spectrosc.* **1987**, 2, 24.

52. Oechsner, H.; *Appl. Phys.* **1975**, 8, 185.

53. Barshick, C. M. Ph.D Dissertation; University of Virginia (1990).

54. Loving, T. J.; Harrison, W. W. *Anal. Chem.* **1983**, 55, 1526.

55. Larkins, P. L. *Spectrochim. Acta* **1991**, 46B, 291.

56. Laegreid, N.; Wehner, G. K. *J. Appl. Phys.* **1961**, 32, 365.

57. Avni, R. Applied Atomic Spectroscopy;. Grove; E.L.; Ed. Plenum Press: New York, 1978.

58. Dahlgren, S. D.; MacClanahan, E. D. *J. Appl. Phys.* **1972**, 43, 1514.

59. Shimizu, R.; Saeki, N. *Surf. Sci.* **1977**, 62, 751.

60. Coburn, J. W., *J. Vac. Sci. Technol.* **1976**, 13, 1037.

61. Oechsner, H.; Gerhard, W. *Surf. Sci.* **1974**, 44, 480.

62. Gerhard, W.; Oechsner, H. *Z. Physik B*; **1975**, 22, 41..

63. Harrison, W. W.; Hess, K. R.; Marcus, R. K.; King, F. L., *Anal. Chem.* **1986**, 58, 341 A.

64. Oechsner, H. *Plasma Phys.* **1974**, 16, 835.

65. McHugh, J. A. Methods of Surface Analysis, Volume I; Czanderna, A.W., Elsevier: New York, 1975.

66. Cobine, D. C. *Gaseous Conductors*; Dover: New York, 1958.

67. Stedman, D. H; Setser, D. W. *Prog. in Reaction Kinetics* **1971**, 6, 193.

68. Penning, F.M. *Z. Physik*, **1929**, 57, 723.

69. Hess, K. R.; Harrison; W. W. *Anal. Chem.* **1988**, 60, 691.

70. Coburn, J. W. *Rev. Sci. Instr.* **1970**, 41, 1219.

71. Vieth, W.; Huneke, J. C. *Spectrochim. Acta* **1990**, 45B, 941.

72. Eckstein E. W., Coburn, J. W. and Kay, E.; *J. Mass Spectrom. Ion Phys.* **1975**, 17, 129.

73. Coburn, J. W.; Taglauer, E.; Kay E.; *J. Appl. Phys.* **1975**, 45, 1779.

74. Phelps, A. V.; Molnar, J. P. *Phys. Rev.*, **1953**, 89, 1202.

75. Futch A. H.; Grant, F. A. *Phys. Rev.* **1956**, 104, 356.

76. Delcroix, D. L.; Ferreira, C. M.; Richard, A. *Principles of Laser Plasmas*; G.Bekefi, Ed.; Wiley: New York, 1976.

77. Velazco, J. E.; Kolts, J. H.; Setser, D. W. *J. Chem. Phys.* **1978**, 69, 4357.

78. Smith, R. L.; Serxner, D.; Hess, K. R. *Anal. Chem.* **1989**, 61, 1103.

79. Waitlevertch, M. E; Hurwitz, J. K. *Appl. Spectrosc.* **1976**, 30, 510.

80. Glick, M.; Smith, B. W.; Winefordner, J. D. *Anal. Chem.* **1990**, 62, 157.

81. Broekart, J. A. C. *Bull. Soc. Chim. Belg.* **1976**, 85, 471.

82. Dawson, J. B.; Ellis, D. J. *Spectrochim. Acta*, **1967**, 23A, 565.

83. Klingler, J. A.; Savickas, P. J.; Harrison, W. W. J. Am. Soc. Mass Spectrom. **1990**, 1, 138.

84. King, F. L.; Pan, C. *Anal. Chem.* **1993**, 65, 735.

85. Klingler, J. A.; Barshick, C. M.; Harrison, W. W. *Anal. Chem.* **1991**, 63, 2571.

86. Biondi, M. A. *Phys. Rev.* **1952**, 88, 660.

87. Strauss, J. A.; Ferreira, N. P.; Human, H. G. C. *Spectrochim. Acta* **1982**, 37B, 947.

88. Hardy, J. A.; Sheldon, J. W. *J. Appl. Phys.* **1982**, 53, 8532.

89. Muschlitz, E. E.; *Science* **1968**, 159, 599.

90. Wood, R. W. *Phil. Mag.* **1902**, 3, 128.

91. Wood, R. W.; Mohler, F.L. *Phys. Rev.* **1918**, 11, 70.

92. Nichols, E. L.; Howes, H. L. *Phys. Rev.* **1924**, 23, 472.

93. Boers, A. L.; Alkemade, C. T. J.; Smit, J. A. *Physica* **1956**, 22, 358.

94. Omenetto, N.; Winefordner, J. D. *Atomic Fluorescence Spectroscopy with Laser Excitation*; N. Omenetto, Ed.; John Wiley and Sons: New York, 1979.

95. Mansfield, J. M.; Winefordner, J. D. *Anal. Chem.* **1965**, 37(8), 1050.

96. Armentrout, D. N. *Anal. Chem.* **1966**, 38(9), 1236.

97. Klaus, R.; Klin Z. *Chem.* **1966**, 4, 29.

98. Amos, M. D.; Bennett, K. G.; Brodie, K. G.; Lung, P. W. Y.; Matousek, J. P. *Anal. Chem.* **1971**, 43, 211.

99. Dagnall, R. M.; Taylor, M. R. G.; West, T. S. *Lab. Pract.* **1971**, 20, 209.

100. Kirkbright, G. F.; Rao, A. P.; West, T. S. *Anal Letters* **1969**, 2, 465.

101. Dagnall, R. M.; Kirkbright, G. F.; West, T. S.; Wood, R. L. *Anal. Chem.* **1971**, 43, 1765.

102. Cotton, D. H.; Jenkins, D. R. *Spectrochim. Acta* **1970**, 25B, 283.

103. Seliskar, C. J. *Spectrochim. Acta* **1988**, 43B, 51.

104. Boutilier, G. D.; Blackburn, M. B.; Mermet, J. M.; Weeks, S. J.; Haragushi, H. J.; Winefordner, J. D.; Omenetto, N. *Appl. Optics* **1978**, 18, 1804.

105. Omenetto, N.; Winefordner, J. D. *Prog. Anal. At. Spectrosc.* **1971**, 2, 1.

106. Alkemade, C. Th. J. *Appl. Spectrosc.* **1981**, 35, 1.

107. Alkemade, C. Th. J. "Detection of Small Numbers of Atoms and Molecules," in *Analytical Applications of Lasers*; Piepmeier, E.H., Ed.; Wiley Interscience: New York, 1986.

108. Omenetto, N. *Spectrochim. Acta* **1989**, 44B, 131.

109. Winefordner, J. D.; Epstein, M. S. *Phys. Methods of Chem.*; Vol. 3; Chemical Composition and Molecular Structure, Part A; Bryant Rossiter Ed.; John Wiley and Son, Inc.: New York, 1987

110. Butcher, D. J.; Dougherty, J. P.; McCaffrey J. T.; Preli, F. R.; Walton, A. D.;Michel, R. G. *Prog, in Anal. Chem.* **1987**, 10, 4.

111. Butcher, D. *Spectrosc.* **1993**, 8(2), 14.

112. van Loon, J. C. *Anal. Chem.* **1981**, 53, 332A.

113. Winefordner, J.D.; Omenetto, N. "Laser-excited Atomic and Ionic Fluorescence in Flames and Plasmas," in *Analytical Applications of Lasers*; Piepmeier, E.H., Ed.;Wiley Interscience: New York, 1986.

114. Winefordner, J. D.; Petrucci, G. A.; Stevenson, C. L.; Smith, B. W. *J. Anal. At. Spectrom.* **1994**, 9, 131.

115. Smith, B. W.; Womack, J. B.; Omenetto, N.; Winefordner, J. D. *Appl. Spectrosc.* **1989**, 43, 873.

116. Deavor, J. P.; Becerra, E.; Smith, B. W.; Winefordner, J. D. Can. J. Spectrosc. **1993**, 33, 7.

117. Dashin, S. A.; Karpov, A.; Kushlyansky, O. A.; Maytorov, I. A.; Bolshov, M. A.; *Spectochim. Acta B*, **1991**, 46, 467.

118. Bengtson, A. *Spectrochim. Acta B.* **1991**, 40, 631.

119. Mignardi, M. A.; Smith, B. W.; Jones, B. T.; Krupa, R. J.; Winefordner, J. D. Talanta **1989**, 36, 311.

120. Chaung, F. S.; Winefordner, J. D. *Appl. Spectrosc.* **1975**, 29, 412.

121. Bratzel, M. P., Jr; Dagnell, R. M.; Winefordner, J. D. *Anal. Chim. Acta* **1970**, 52, 157.

122. Mattson, W. A.; Bentz, B. L.; Harrison, W. W. *Anal. Chem.* **1976**, 48, 489.

123. *Atomic Transition Probabilities*, NSRDS-NBS22, Washington, D. C., 22nd ed., **1969**, 8, 859.

124. Barnett, W. B.; Kahn, H. L.; *Anal. Chem.* **1972**, 44, 935.

125. Bohm, D.; Gross, E. P. *Phys. Rev.* **1949**, 75, 1864.

126. Adamson, A. W. Physical Chemistry of Surfaces, 3rd ed.; Wiley: New York, 1976.

127. Maitland, G. C.; Rigby, M. Smith, E. B.; Wakeman, W. A. *Intermolecular Forces*, Clarendon Press, Oxford, 1981, Ch. 5.

128. Smithells, C. J. *Metals Reference Book*, 3rd ed; Butterworths & Co.: Washington D.C., 1962, p. 662.

129. J.A. Klingler, C.M. Barshick, and W.W. Harrison *Analytical Chemistry* **1991**, 63, 2571-2576.

130. Klinger, J. A.; Savickas, P. J.; Harrison W. W. *J. Am. Soc. Mass Spectrom.* **1990**, 1, 138.

131. Strauss, J. A.; Ferreira, N. P.; Human, H. G. C. *Spectrochim. Acta* **1982**, 37B, 947.

132. Glick, M.; Smith, B. W.; Winefordner, J. D. *Anal. Chem.* **1990**, 62, 157.

133. Walden, W. O.; Harrison W. W.; Smith, B. W.; Winefordner, J. D. *J. Anal. Atom. Spectrosc.* **1994**, 9, 1039.

134. Mixon, P. D.; Griffin, S. T.; Williams Jr., J. C.; Cai, X. J.; Williams, J. C. *J. Anal. Atom. Spectrosc.* **1994**, 9, 697.

135. Dawson, J. B.; Ellis, *Spectrochim. Acta* **1967**, 23A, 565.

136. Hang, W.; Wang, X.;Yang, P.; Su, Y.; Huang, B. *Rapid Comm. in Mass Spectrom.* **1994**, 8, 590.

137. Bohm, D.; Gross, E. R. *Phys. Rev.* **1949**, 75, 1864.

138. Farnsworth, P. B.; Walter, J. P. *Spectrochim. Acta* **1982**, 37B, 773.

139. Mermet, J. M. *In Inductively Coupled Plasma Emission Spectroscopy, Part 2, Applications and Fundamentals*; P. W. J. M. Boumans, Ed.; John Wiley and Sons: New York, 1987, ch. 10.

140. Ohorodnik, S. K.; Harrison, W. W. *J. Atom. Anal. Spectros.* **1994**, 9, 991.

141. Ingeneri, K. Unpublished results, University of Florida, Gainesville, Fl., 1995.

142. Barrow, G. M. *Physical Chemistry*; McGraw-Hill Co.: New York, 1988.

BIOGRAPHICAL SKETCH

William Walden was born in Arlington Heights, Ilinois on June 6, 1968. His college career began at Florida State University in 1986. He transferred to the University of Florida in 1990 and received his Bachelor of Science degree in chemistry in December 1991. In January, 1992 he became a shared graduate student at the University of Florida for Dr. J. D. Winefordner and Willard W. Harrison. He completed his graduate career with a Doctor of Philosophy degree in December 1995.

I certify that I have read this study and that in my opinion it conforms to acceptable standards of scholarly presentation and is fully adequate, in scope and quality, as a dissertation for the degree of Doctor of Philosophy.

James D Winefordner

James D. Winefordner, Co-Chair
Graduate Research Professor of Chemistry

I certify that I have read this study and that in my opinion it conforms to acceptable standards of scholarly presentation and is fully adequate, in scope and quality, as a dissertation for the degree of Doctor of Philosophy.

Willard W. Harrison, Co-Chair
Professor of Chemistry

I certify that I have read this study and that in my opinion it conforms to acceptable standards of scholarly presentation and is fully adequate, in scope and quality, as a dissertation for the degree of Doctor of Philosophy.

Robert T. Kennedy
Assistant Professor of Chemistry

I certify that I have read this study and that in my opinion it conforms to acceptable standards of scholarly presentation and is fully adequate, in scope and quality, as a dissertation for the degree of Doctor of Philosophy.

John R. Eyler

John R. Eyler
Professor of Chemistry

I certify that I have read this study and that in my opinion it conforms to acceptable standards of scholarly presentation and is fully adequate, in scope and quality, as a dissertation for the degree of Doctor of Philosophy.

Neil Sullivan
Professor of Physics

This dissertation was submitted to the Graduate Faculty of the Department of Chemistry in the College of Liberal Arts and Sciences and to the Graduate School and was accepted as partial fulfillment of the requirements for the degree of Doctor of Philosophy.

December, 1995

Dean, Graduate School